

Copyright
by
Abhishek Gaurav
2010

**The Thesis Committee for Abhishek Gaurav
Certifies that this is the approved version of the following thesis:**

**Ultra Light Weight Proppants in
Shale Gas Fracturing**

**APPROVED BY
SUPERVISING COMMITTEE:**

Supervisor:

Kishore K. Mohanty

Mukul M. Sharma

**Ultra Light Weight Proppants
in Shale Gas Fracturing**

by

Abhishek Gaurav, B. Tech

Thesis

Presented to the Faculty of the Graduate School of

The University of Texas at Austin

in Partial Fulfillment

of the Requirements

for the Degree of

Masters of Science in Engineering

The University of Texas at Austin

December 2010

Dedication

To my family and friends

Acknowledgements

I would like to thank my advisor Dr. Kishore K. Mohanty for his help and guidance in completing my thesis. I am grateful for his patience and kindness during the course of the project. He taught me the ability to conduct research independently, which is an invaluable gift for me.

I would also like to thank Dr. A. Daneshy, Dr. Qi Qu, Dr. T. J. Pisklak for their timely advice and direction in completing this project. I received valuable input from them throughout the course of this project.

Finally I would like to thank Dr. Eric Dao for his constant help and support in conducting my experiments.

December 3, 2010

Abstract

Ultra Light Weight Proppants in Shale Gas Fracturing

Abhishek Gaurav, M. S. E.

The University of Texas at Austin, 2010

Supervisor: Kishore K. Mohanty

Abstract: The goal of the present work is to improve shale reservoir stimulation treatment by using ultra light weight proppants in fracturing fluids. Slickwater has become the most popular fracturing fluid for fracturing shales in recent times because it creates long and skinny fractures and it is relatively cheap. The problem with slickwater is the high rate of settling of common proppants, e.g. sand, which results in propped fractures which are much smaller than the original fractures. Use of gels can help in proppant transport but introduce large formation damage by blocking pores in nano-darcy shales. Gel trapping in the proppant pack causes reduction in permeability of the proppant pack. The light weight proppants which can easily be transported by slickwater and at the same time be able to provide enough fracture conductivity may solve this problem. Three ultra light weight proppants (ULW1, ULW2, and ULW3) have been studied. The

mechanical properties of the proppant packs as well as single proppants have been measured. Conductivity of proppant packs has been determined as a function of proppant concentration and confining stress at an average Barnett shale temperature of 95°C. The crush strengths of all the three proppant packs are higher than typical stresses encountered (e.g., Barnett). ULW1 and ULW2 are highly deformable and do not produce many fines. ULW3 has a higher Young's modulus and produces fines. Conventionally, the proppant conductivity decreases with decreasing proppant concentration and increasing confining stress. But in cases of ULWs, for a partial monolayer, conductivity can be as large as that of a thick proppant pack. The settling velocity is the lowest for ULW1, intermediate for ULW2 and the highest for ULW3. This work contributes new mechanical, conductivity, and settling data on three ultra light weight proppants. Application of light weight proppants in stimulation treatments in shale reservoirs can lead to large propped fractures, which can improve the productivity of fractured shale reservoirs.

Table of Contents

List of Tables	x
List of Figures	xi
1. Introduction.....	1
1.1. Ultra Light weight Proppants	2
1.2. Objective.....	2
2. Literature Review.....	3
2.1. Fracturing Aspects.....	3
2.2. Proppants and Fracturing.....	7
2.2.1. Slickwater Fracturing	7
2.2.2. Partial Monolayers	12
2.2.3. Ultra light weight proppants.....	18
2.2.4. Conclusions	20
3. Approach and Methodology	22
3.1. Estimation of physical properties	22
3.1.1. Bulk Density.....	22
3.1.2. Absolute Density	22
3.1.3. Sphericity	22
3.1.4. Sieve-size distribution	23
3.2. Estimation of mechanical properties	24
3.2.1. Strength	24
3.2.2. Crush Test	24
3.2.3. Conductivity Test	24
4. Description and Application of Equipment and Processes	25
4.1. Estimation of physical properties	25
4.1.1. Bulk Density.....	25
4.1.2. Absolute Density	27
4.1.3. Strength and Crush Test	29

4.1.4.	Conductivity Test	30
5.	Results	33
5.1.	Absolute Density, Bulk Density, Porosity and Sphericity.....	33
5.2.	Size Distribution	37
5.3.	Crush Test.....	37
5.4.	Strength Test of Single Proppant Particle.....	45
5.4.1.	ULW 1	45
5.4.2.	ULW 2	47
5.4.3.	ULW 3	48
5.5.	Deformability.....	50
5.6.	Conductivity Tests	52
6.	Conclusions and Recommendations for Future Work	57
6.1.	Conclusions	57
6.2.	Recommendations for future work	58
	References	59
	Vita.....	62

List of Tables

Table 5.1 Tabular representation of bulk density, nominal density, porosity and sphericity for the three proppants being studied	33
Table 5.2 Tabular representation of fines formation and Young's modulus value for proppant packs for various cases	41

List of Figures

Figure 2.1 McGuire and Sikiora's producing-rate folds-of-increase curves (1960).....	3
Figure 2.2 Productivity-index-ratio increase from fracturing steady-state flow, vertical propped fractures (Tinsley et al., 1969).....	4
Figure 2.3 Producing-rate type curves with propped vertical fractures-transient flow, constant wellbore pressure (Agarwal et al., 1979).....	5
Figure 2.4 Producing-rate type curves with propped vertical fractures-transient flow, constant flow-rate (Cinco et al., 1978).....	6
Figure 2.5 Fracture width comparison for various fracturing treatments (Palisch and Vincent, 2008).....	8
Figure 2.6 Proppant settling in freshwater for various proppants (Aboud and Melo, 2007).....	9
Figure 2.7 Terminal velocity of different sized particles predicted by Stoke's equation and corrected for inertial effects in 1 cp fluid.....	10
Figure 2.8 Terminal velocity of different sized particles predicted by Stoke's equation and corrected for inertial effects in 10 cp fluid.....	11
Figure 2.9 Correlations for effect of solids concentration on settling velocity	11
Figure 2.10 Wall effects using the average velocity	12
Figure 2.11 Proppant particles in contact with each other in a full mono-Layer and sparsely distributed particles in a partial mono-layer (Brannon and Malone, 2004).....	13
Figure 2.12 Darin and Huitt's work on monolayers and thick packs of 20/40 Sand.....	13
Figure 2.13 Weight percent crushed for various concentrations at 6000 psi stress (Howard and Fast, 1970).....	14
Figure 2.14 Full monolayers of various proppant being tested for conductivity at 1000 psi stress (Wang and Fredd, 2008).....	15
Figure 2.15 Base line conductivity vs. stress for a thick multi layered pack and a partial monolayer for 16/25 ULW 1.25 at 150°F	16
Figure 2.16 Conductivity vs. proppant concentration for various sizes of Brady sand at 1,000 psi closure stress and 100°F	16
Figure 2.17 Conductivity vs. proppant concentration for 8/12 Brady sand at various closure stress	17
Figure 2.18 Conductivity vs. proppant concentration at 1000 psi closure stress comparing Brady sand and ULW 1.25	17
Figure 2.19 Conductivity vs. proppant concentration for 8/12 ULW 1.25 at different temperatures.....	18
Figure 2.20 Simulation of Ottawa sand proppant placement at pumping rate of 80 bpm using Mfrac simulator	19
Figure 2.21 Simulation of light weight proppant placement at pumping rate of 80 bpm using Mfrac simulator	20
Figure 3.1 Chart for visual estimation of sphericity and roundness, X axis-roundness and Y axis-sphericity	23
Figure 3.2 Riley Sphericity: $\Psi_R = (D_i/D_c)^{0.5}$	23

Figure 4.1 Bulk density measurement for ULW 1 in a graduated glass cylinder	25
Figure 4.2 Bulk density measurement for ULW 2 in a graduated glass cylinder	26
Figure 4.3 Bulk density measurement for ULW 3 in a graduated glass cylinder	26
Figure 4.4 Absolute density measurement for ULW 1 in a graduated glass cylinder using propyl alcohol	27
Figure 4.5 Absolute density measurement for ULW 2 in a graduated glass cylinder using propyl alcohol	28
Figure 4.6 Absolute density measurement for ULW 3 in a graduated glass cylinder using propyl alcohol	28
Figure 4.7 Tool used for testing strength or proppant in a HUMBOLDT strength test machine	29
Figure 4.8 API conductivity Cell under stress inside an oven maintained at 95°C	31
Figure 5.1 Two-dimensional close up image of ULW 1	34
Figure 5.2 Two-dimensional close up image of ULW 2	35
Figure 5.3 Two-dimensional close up image of ULW 3	35
Figure 5.4 Sphericity and Roundness distribution for three types of proppants ULW 1, ULW 2 and ULW 3	36
Figure 5.5 Size Distribution of the three types of proppants	37
Figure 5.6 Maximum possible values for horizontal stresses in Barnett shale, Haynesville shale and Woodford shale	40
Figure 5.7 Stress vs. Strain curve for ULW 1 at ~95°C	42
Figure 5.8 Stress vs. Strain curve for ULW 1 at ~25°C	42
Figure 5.9 Stress vs. Strain curve for ULW 2 at ~95°C	43
Figure 5.10 Stress vs. Strain curve for ULW 2 at ~25°C	43
Figure 5.11 Stress vs. Strain curve for ULW 3 at ~95°C	44
Figure 5.12 Stress vs. Strain curve for ULW 3 at ~25°C	44
Figure 5.13 Strength test for single particles of ULW 1 at ~95°C	46
Figure 5.14 Strength test for single particles of ULW 1 at ~25°C	46
Figure 5.15 Strength test for single particles of ULW 2 at ~95°C	47
Figure 5.16 Strength test for single particles of ULW 2 at ~25°C	48
Figure 5.17 Strength test for single particles of ULW 3 at ~95°C	49
Figure 5.18 Strength test for single particles of ULW 3 at ~25°C	49
Figure 5.19 Elastic modulus of ULW 1 at ~25°C	51
Figure 5.20 Elastic modulus of ULW 2 at ~25°C	51
Figure 5.21 Elastic modulus of ULW 3 at ~25°C	52
Figure 5.22 Fracture conductivity for ULW 1	54
Figure 5.23 Fracture conductivity for ULW 2	55
Figure 5.24 Fracture conductivity for ULW 3	56

1. Introduction

The Barnett shale, since its discovery, is being produced from more than 8,000 wells today (Wang et al., 2008). The success of gas production from Barnett can be attributed to horizontal drilling and hydraulic fracture stimulation. But there were many lessons learned while exploiting Barnett shale gas reserves. Fracture stimulation in shale gas reserves is not the same as fracturing typical gas reservoirs. These shale gas formations have permeability of the order of 10^{-9} Darcies. Therefore, hydraulic fractures need to be long and extensive to maximize reservoir contact.

Silica sand has been the most commonly used proppant. The ready availability and lower cost makes it attractive for stimulation treatments. If conventional proppants, like Ottawa sand (specific gravity = 2.65), are used in typical fracturing fluid like slick water, proppants settle during the fracturing process before reaching the end of the long fractures, due to which a lot of producible surface area is lost after stimulation. Re-stimulation is an option, but it makes the process more expensive. Sintered bauxite, another commonly used proppant material, is significantly stronger than sand and is used in deeper formations where high fracture closure stresses severely crush sand. The fracturing fluids can carry the conventionally used heavy proppants if they are made more viscous by using polymers in them. This viscosity can be further increased by cross-linking these polymers. However, when the fracturing fluid is very viscous, the resulting fractures are short and wide, and do not reach a major part of the producible area. Also, the large polymer molecules can plug the fracture faces of these extremely low permeability shales.

1.1. ULTRA LIGHT WEIGHT PROPPANTS

One way to overcome these problems is to use light weight proppants which can be transported by a less complex fracturing fluid and at the same time, be strong enough to withstand reservoir stresses. The result of multi-disciplined research and development efforts created a new class of ultra-light weight proppants, having both low specific gravity and requisite mechanical strength (Brannon and Malone). These light weight proppants could effectively be used with simpler fracturing fluids, like slick water. The first generation of ULWPs were resin-impregnated and coated, sized, chemically modified walnut hulls, having a specific gravity of 1.25; less than half that of sand (2.65). These proppant particles could achieve neutral buoyancy in fracturing water. Settling rates for these first generation ULWPs were 24% that of similarly sized sand. Another type of ULWPs developed around the same period were resin coated ceramic proppants, which had a specific gravity of 1.75; much lighter than sand particles. In terms of transportability, these proppants showed more promise with slickwater than conventional sand or sintered bauxite (sp. gr. ~ 3.6). Typical fracturing processes are extremely water intensive. Once the fracturing job is over, there are other issues with the disposal of the fracturing fluids. The proppants being light also gives us an option of using fracturing foams (mixture of gas and liquid phase), thereby reducing the usage of water.

1.2. OBJECTIVE

This work focuses on three ultra light weight proppants, ULW-1 (polymeric), ULW-2 (resin coated and impregnated ground walnut hull) and ULW-3 (resin coated ceramic), supplied by BJ services. The physical properties of these proppants have been evaluated along with their mechanical properties. These tests are followed up with conductivity measurements of various concentrations of proppants at different stress levels.

2. Literature Review

2.1. FRACTURING ASPECTS

Various graphical/computerized methods have been developed to estimate the effects of fracture length and fracture conductivity on well productivity increase for both low permeability and high permeability reservoirs. For high permeability reservoirs, where steady-state (or pseudo steady state) flow develops relatively quickly, methods provided by McGuire and Sikora (1960), can be used to estimate the productivity increase from a fracturing treatment. Figure 2.1 and Figure 2.2 indicate productivity increase as a function of various fracturing parameters. If the fracturing parameters can be controlled using a systematic fracture design, productivity can be increased up to a certain extent.

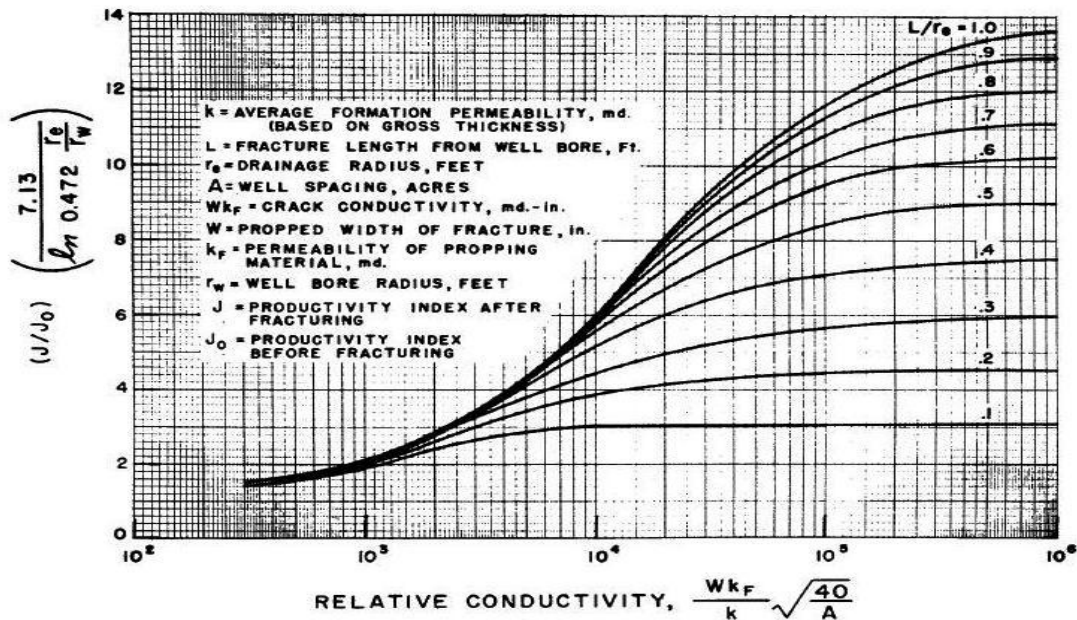


Figure 2.1 McGuire and Sikora's producing-rate folds-of-increase curves (1960)

In Figure 2.1, it is shown that increasing the value of fracture conductivity can increase the productivity of the well significantly only if the fracture penetration ($L/R_e = \text{Fracture half-length/Reservoir Radius} > 0.2$) is high enough. As fracture length increases, productivity enhancement increases. For lower fracture penetration (around 0.1 or less), even a significant increase in fracture conductivity, helps in enhancing the productivity only by a factor of 3. This graph also shows that the productivity enhancement does not increase with the increase in conductivity beyond a certain value of fracture conductivity (or relative conductivity) for a given fracture length.

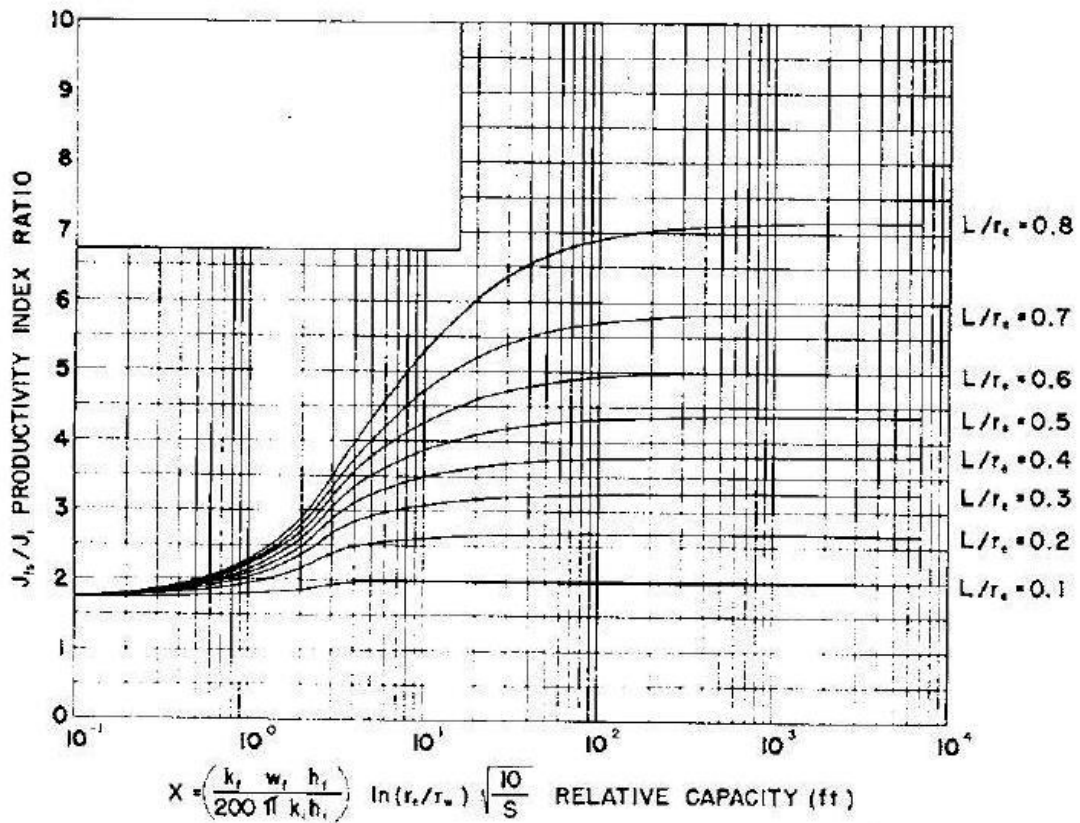


Figure 2.2 Productivity-index-ratio increase from fracturing, steady-state flow, vertical propped fractures (Tinsley et al., 1969)

Figure 2.2 indicates for a high L/Re , a good stimulation treatment (high fracture conductivity) value can stimulate the productivity up to 8 times the original productivity.

These methods do not apply to low permeability reservoirs because, for low permeability reservoirs, flow remains in transient state throughout the major portion of well's life. Agarwal et al. (1979) and Cinco et al. (1978) developed methods for evaluation of increase in productivity through fracturing treatments for low permeability reservoirs. Figure 2.3 indicates the plot developed for the case of constant wellbore pressure system. Figure 2.4 indicates the same plot developed for constant flow rate system.

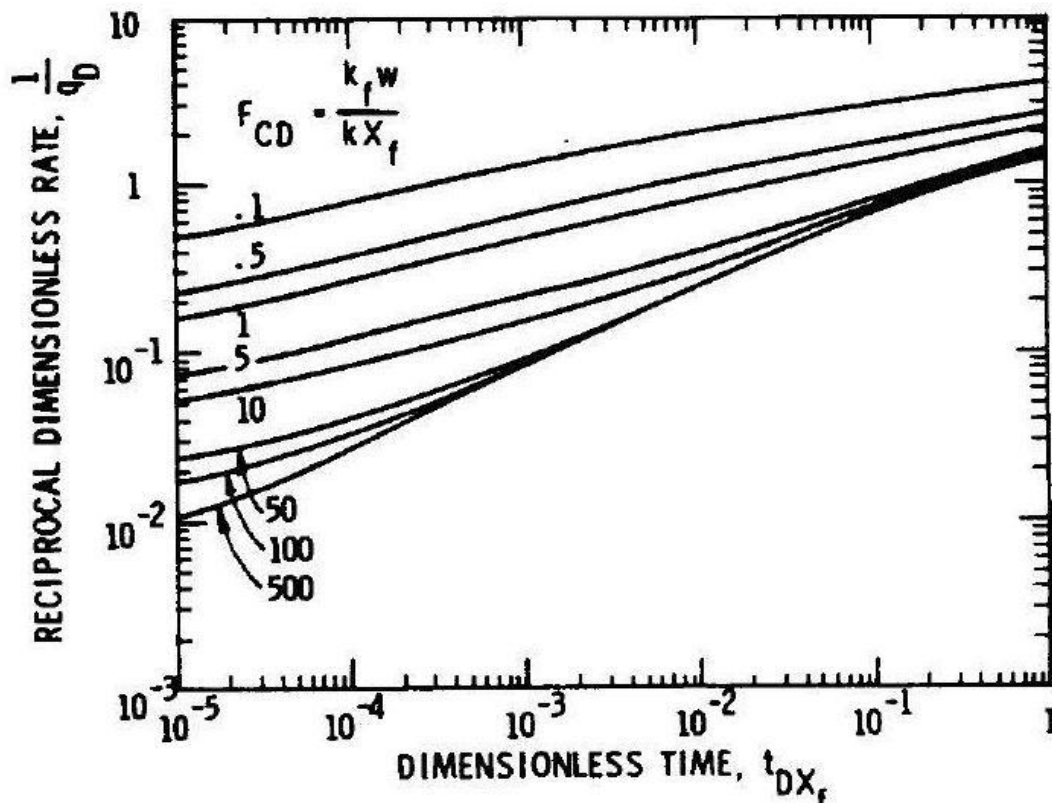


Figure 2.3 Producing-rate type curves with propped vertical fractures-transient flow, constant wellbore pressure (Agarwal et al., 1979)

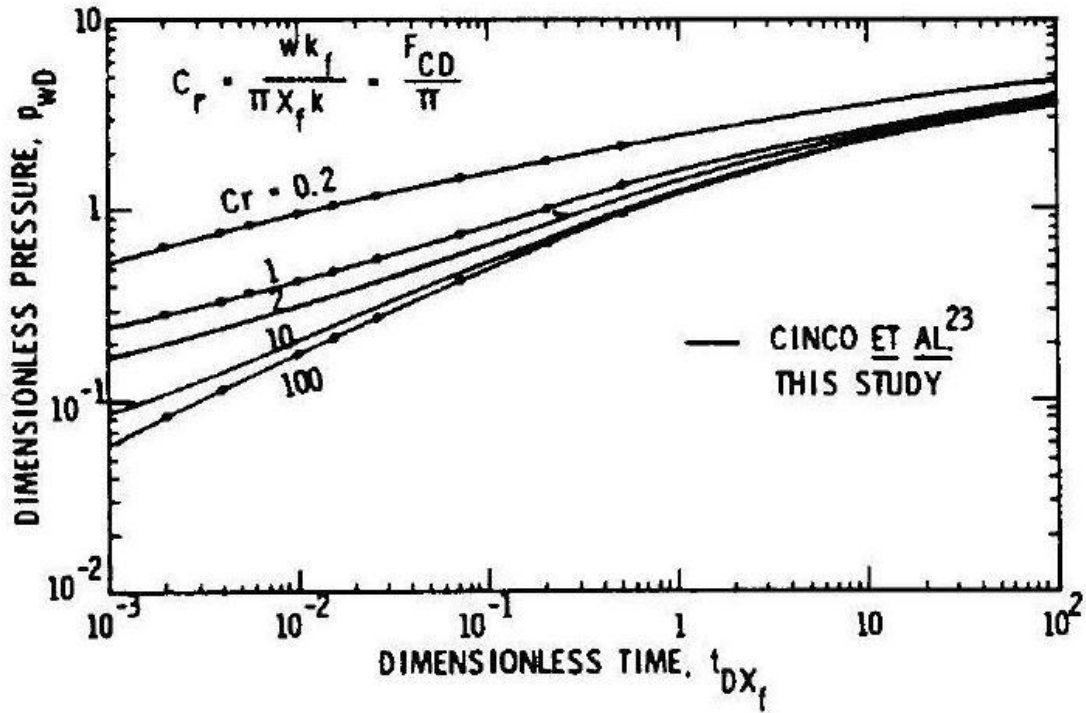


Figure 2.4 Producing-rate type curves with propped vertical fractures-transient flow, constant flow-rate (Cinco et al., 1978)

The ratio of (fracture conductivity)/ (reservoir permeability x fracture half length) i.e., dimensionless fracture conductivity, is a key parameter in these plots. It should be noticed, value for this dimensionless parameter can be high for a low permeability reservoir even when the fracture conductivity is small (of the order of 1 mD-ft). From figures 2.3 and 2.4, for any stimulation treatment, higher dimensionless fracture conductivity gives a higher cumulative production over time (or a lower flowing wellbore pressure), but production does not increase much beyond a dimensionless fracture conductivity of 10. Along with fracture penetration, fracture conductivity plays a pivotal role in enhancing production from any fracturing treatment.

2.2. PROPPANTS AND FRACTURING

Conventional wisdom suggests, stronger the proppant, higher is its density (Rickards et al., 2003). It is difficult to place heavier proppants efficiently in between the fracture faces in long fractures. Rickards and Brannon (2003) conducted a series of experiments testing the utility of lower density proppants under various stress conditions. Efforts in the past in this direction led to the conclusion, that, light weight proppants cannot even maintain sufficient conductivity at a stress level as low as 1000 psi. But with increased usage of slickwater or foam fracturing, the necessity of using ‘easy to transport’ proppants in particular stimulation treatments has risen.

2.2.1. Slickwater Fracturing

Palisch and Vincent (2008) in their works have highlighted the importance of slickwater fracturing treatments. More than 30% of stimulation treatments in 2004 have been slickwater fracturing (Schein, 2005). Slickwater fracturing, as defined by Schein, is a fracture treatment that utilizes a large volume of water to create an adequate fracture geometry and conductivity to obtain commercial production from low perm, large net pay reservoirs. These reservoirs come broadly in the area of Coal Bed Methane, Tight Gas Sands and Shale Gas Plays. The most desirable fracture system in these reservoirs is long and narrow extending to a wider area. The most important slickwater fracturing benefits lie in, reduced gel damage, cost containment, higher stimulated reservoir volume and better fracture containment. But concerns come along with the benefits of using slickwater treatments. The foremost would be poor proppant transport, followed by excessive usage of water and narrower fracture widths.

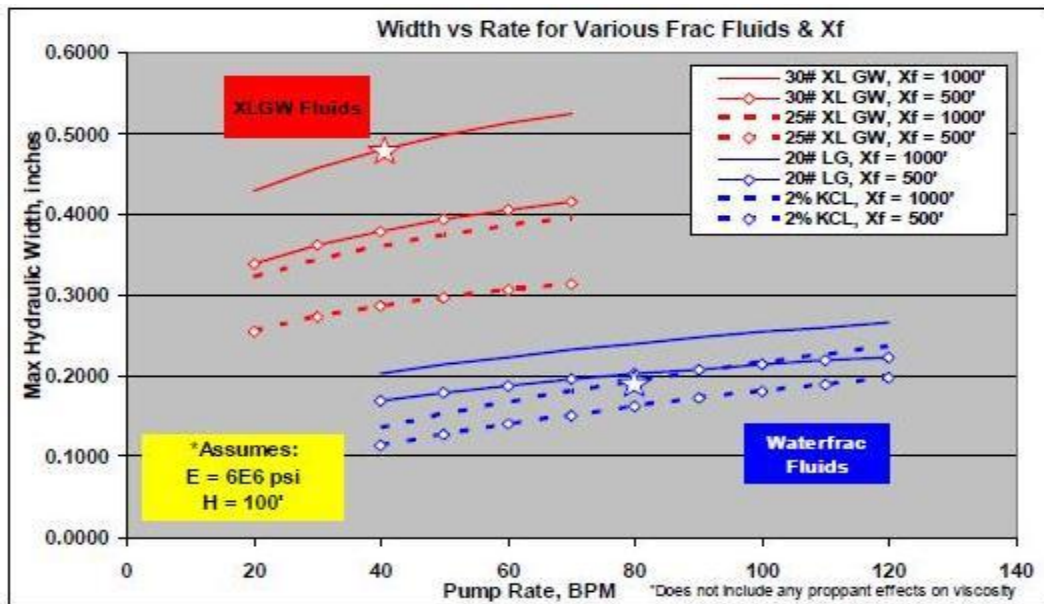


Figure 2.5 Fracture width comparison for various fracturing treatments (Palisch and Vincent, 2008)

Figure 2.5 clearly indicates the decrease in fracture width, once we switch from cross-linked gels to slickwater. But this might be a blessing in disguise for low perm reservoirs. In a nano-darcy permeability reservoir, a long-extensive-wide network of fracture system is desired. With such a fracture system our SRV (stimulated reservoir volume) would be greater than usual. Bigger the SRV, higher is the production from shale wells. To create such a fracture system, a less viscous fracturing fluid like slickwater (unlike cross linked gels) is needed, which can effectively create thin fractures distributed over a wider area. But, proppants should be properly placed throughout the fracture network system before the fracturing fluid is withdrawn. If there are proppants available, which are easy to transport throughout the fracture network with slickwater, possibility of their usage should be looked into.

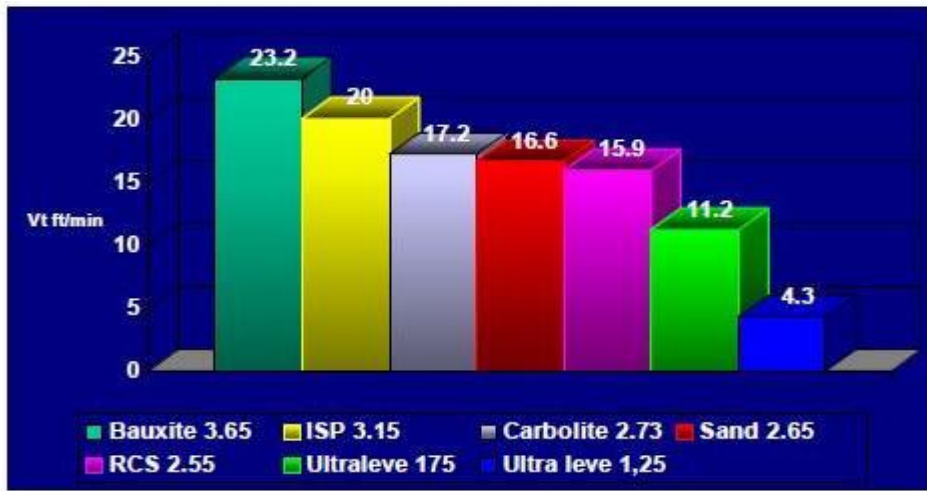


Figure 2.6 Proppant settling in freshwater for various proppants (Aboud and Melo, 2007)

Aboud and Melo (2007) compared the static settling rates of various proppants in freshwater based on Stoke's law (Figure 2.6),

$$V_s = ((\rho_p - \rho_f)(gd_p^2)) / (18\mu) \quad (2.1)$$

where, V_s is the Stoke's settling velocity of a single particle, ρ_p and ρ_f are the density of the particle and the suspending fluid, respectively, d_p is the diameter of the particle, g is acceleration due to gravity and μ is the viscosity of the fluid.

Stokes law has many simplifying assumptions. For Example,

- Fluid must be stagnant
- Absence of "wall effects"
- Proppant particles are perfectly spherical
- Particles fall gradually (laminar flow)
- Absence of inter-particle contact

In spite of these assumptions, Stoke's law helps us to compare the relative settling rate of various proppants based on their density/size and density/viscosity of the fluid (Palisch and Vincent, 2008). This settling velocity is applicable only for small particles Reynolds numbers ($Re_p < 2$) settling in static fluid when wall effects are not important (Asmolov, 2002). For larger Reynolds numbers, settling velocity is affected by the turbulent wakes generated behind the particle. To account for this, Stokes law has been corrected as,

$$V_{Re} = V_s f(Re_p) \quad (2.2)$$

As indicated in Figure 2.7 and Figure 2.8, the creation of wakes due to higher Reynolds number resulted in decrease in settling velocity.

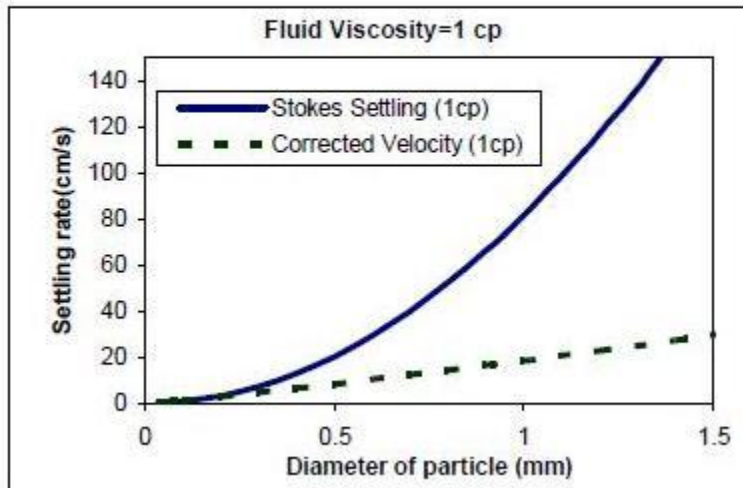


Figure 2.7 Terminal velocity of different sized particles predicted by Stoke's equation and corrected for inertial effects in 1 cp fluid

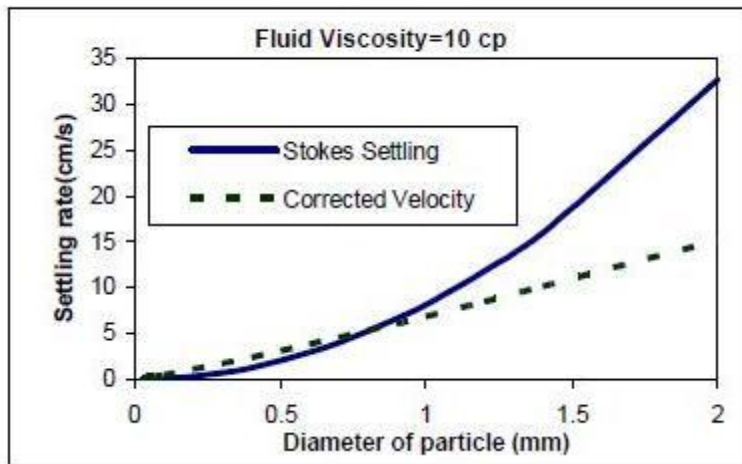


Figure 2.8 Terminal velocity of different sized particles predicted by Stoke's equation and corrected for inertial effects in 10 cp fluid

These results are applicable to single particles and cannot be applied to proppant slurries which are pumped during any fracturing treatment. Gadde et al. (2004) included the effect of proppant concentration on settling which is shown in Figure 2.9. The overall effect of higher proppant concentration resulted in reduction of settling.

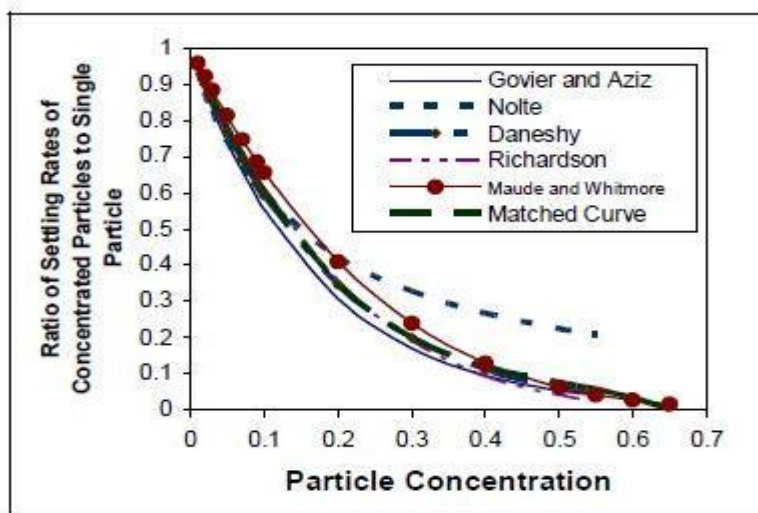


Figure 2.9 Correlations for effect of solids concentration on settling velocity

Gadde et al. (2004) studied the effect of fracture width on settling velocities and found out the modified stokes settling velocity also depends on ratio of the radius of the particle to the width of the slot, guided by equation 2.3,

$$V_w = V_s \left[0.563 \left(\frac{a}{l} \right)^2 - 1.563 \left(\frac{a}{l} \right) + 1 \right] \quad (2.3)$$

where, a is the radius of the sphere, l is the distance of the centre of sphere to either wall, V_s is the stokes settling velocity and V_w is the modified settling velocity which includes the wall effects. Figure 2.10 shows the wall effects tend to reduce settling of proppant particles.

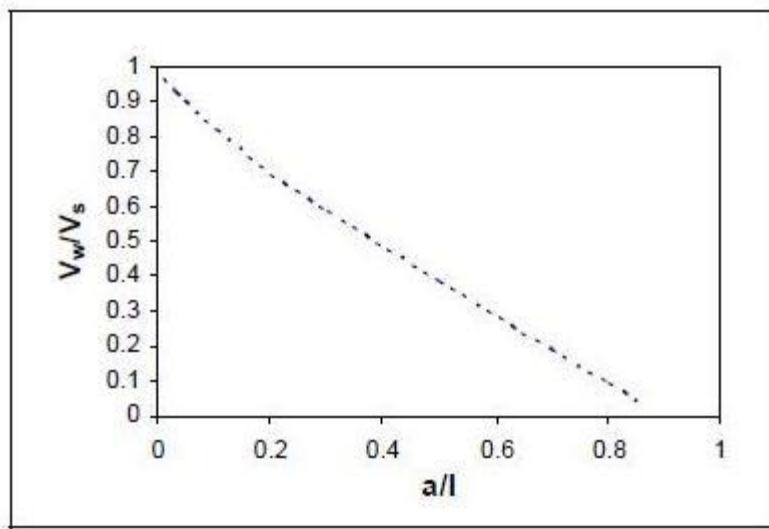


Figure 2.10 Wall effects using the average velocity

2.2.2. Partial Monolayers

Darin and Huitt (1959) introduced the concept of partial monolayers which is shown in the Figure 2.11.

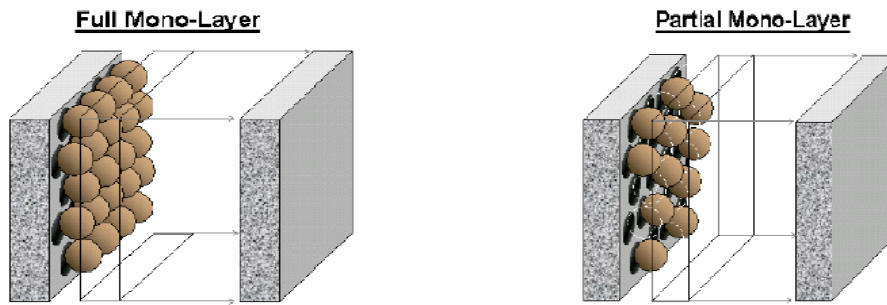


Figure 2.11 Proppant particles in contact with each other in a full mono-Layer and sparsely distributed particles in a partial mono-layer (Brannon and Malone, 2004)

Their reasoning for the success of a partial monolayer was attributed to possibility of flow through open spaces around the sparsely distributed proppant particles.

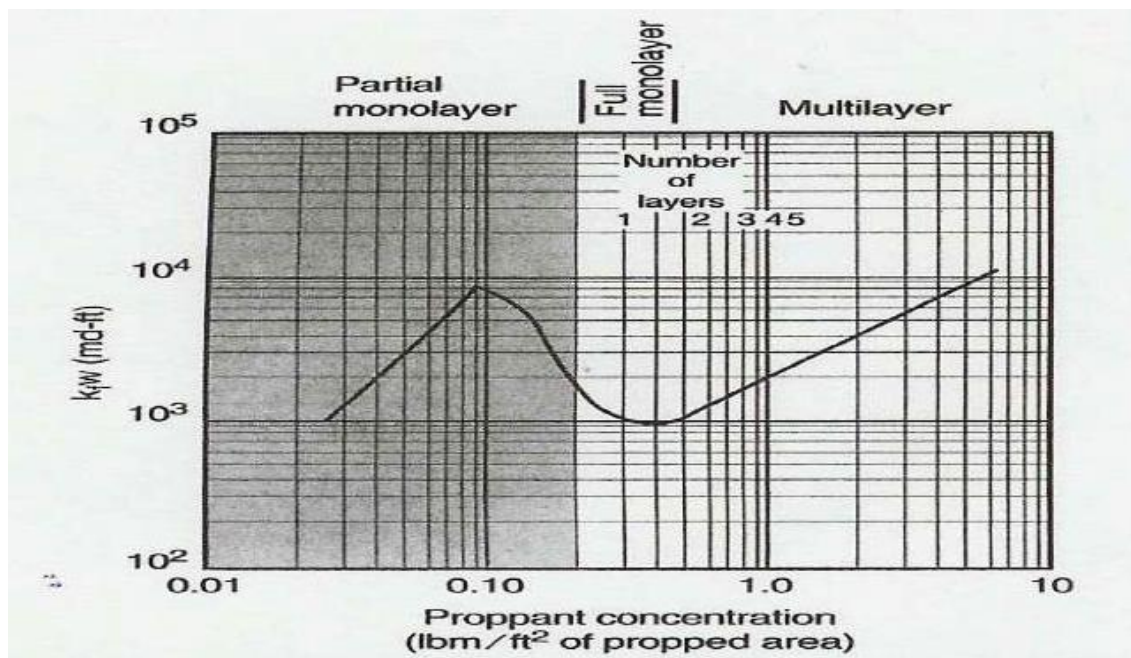


Figure 2.12 Darin and Huitt's work on monolayers and thick packs of 20/40 Sand

But, doubts on uniform distribution of these proppants, their crush strength and embedment into the fracture faces, made this concept unpopular. Howard and Fast (1970) tried to determine the percent of proppants crushed when used as a full-monolayer. They

tested various concentrations of three different 20/40 proppants (resin coated sand, light weight ceramic and white sand) and tried to determine the amount of fines formed for each of them at 6000 psi stress, the results of which are shown in the Figure 2.13.

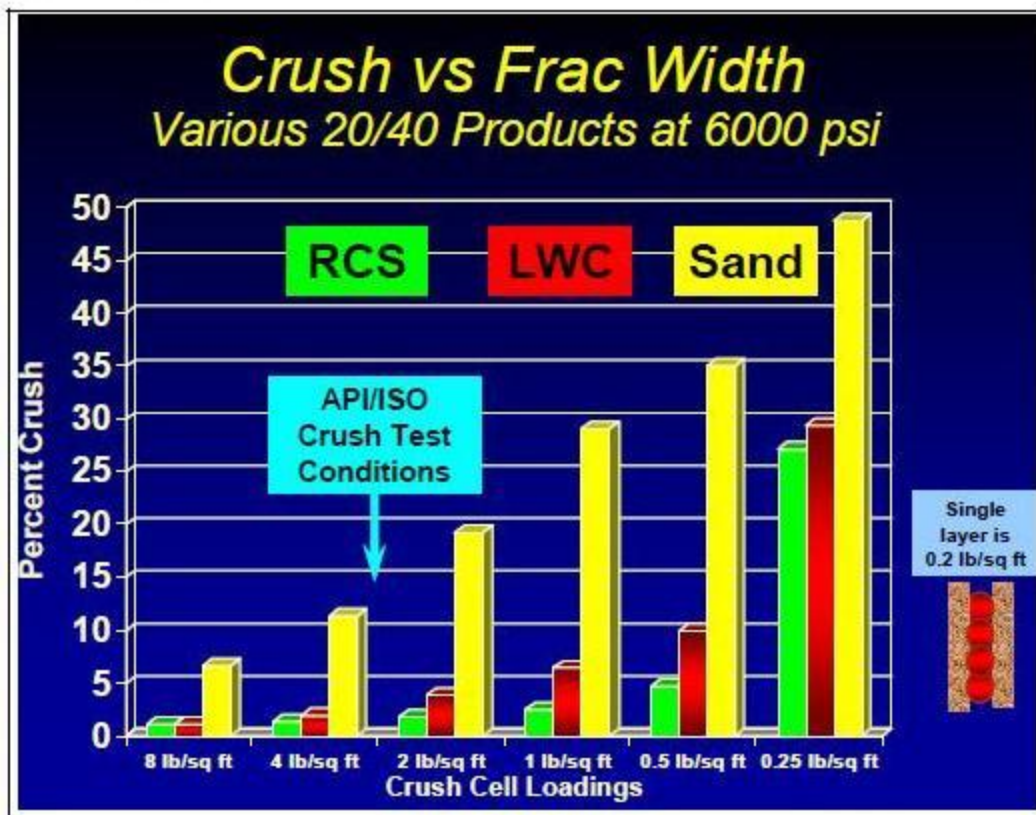


Figure 2.13 Weight percent crushed for various concentrations at 6000 psi stress (Howard and Fast, 1970)

If the success of proppant pack is attributed to less crushing of the pack, then, it is clear that at around a concentration of 0.2 lbm/ft² (a monolayer) this proppant is a complete failure at 6000 psi stress. Light weight proppants are needed that do not form much fines at a high confining stress.

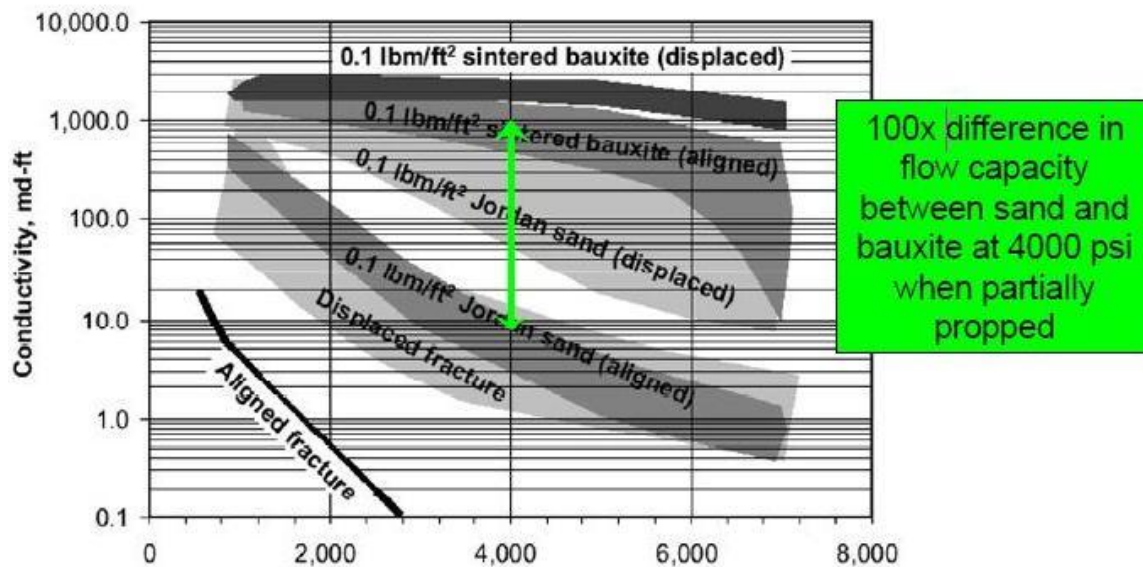


Figure 2.14 Full monolayers of various proppant being tested for conductivity at 1000 psi stress (Wang and Fredd, 2008)

Fredd et al. (2008) showed (Figure 2.14), how there can be a two-order magnitude difference in conductivity when using different materials for full monolayers. High strength material like sintered bauxite full monolayer gives 100 times more conductivity than monolayer of white sand at a stress level of 4000 psi. Sintered bauxite is heavier than even conventional proppant (sand), which means, its monolayer placement with slickwater is doubtful.

Brannon and Malone (2004) measured the conductivity of differently sized sand proppant particles and ULW 1.25 (resin coated and impregnated light weight proppant) proppant particles at different temperatures. They used sandstone cores enclosing proppant pack. In Figure 2.15, conductivity results for 16/25 ULW 1.25 is plotted. The conductivity plot for a partial monolayer runs almost parallel to the conductivity plot for a thick pack of the same proppant with an offset of around 1000 mD-ft.

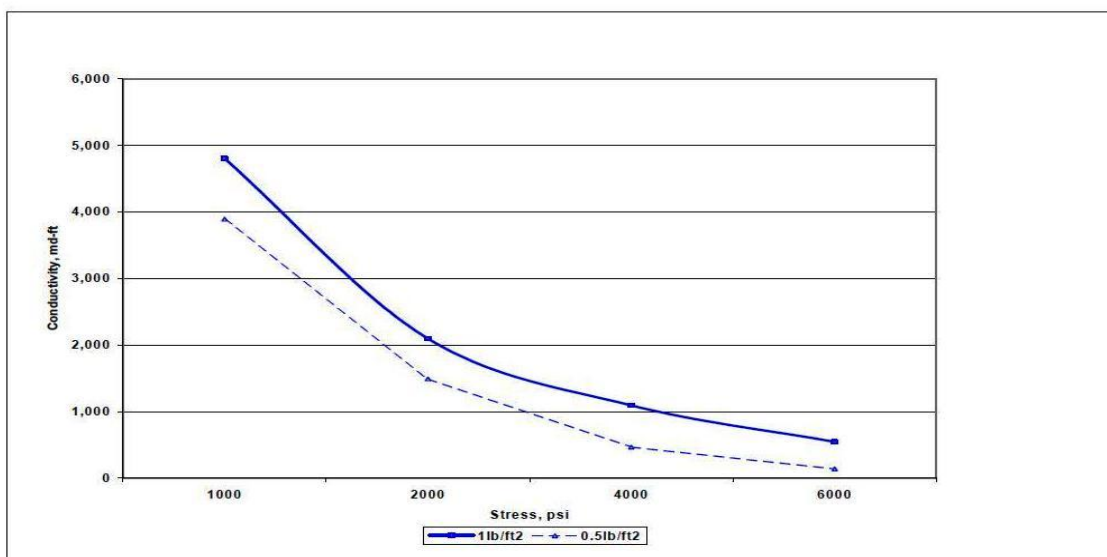


Figure 2.15 Base line conductivity vs. stress for a thick multi layered pack and a partial monolayer for 16/25 ULW 1.25 at 150°F

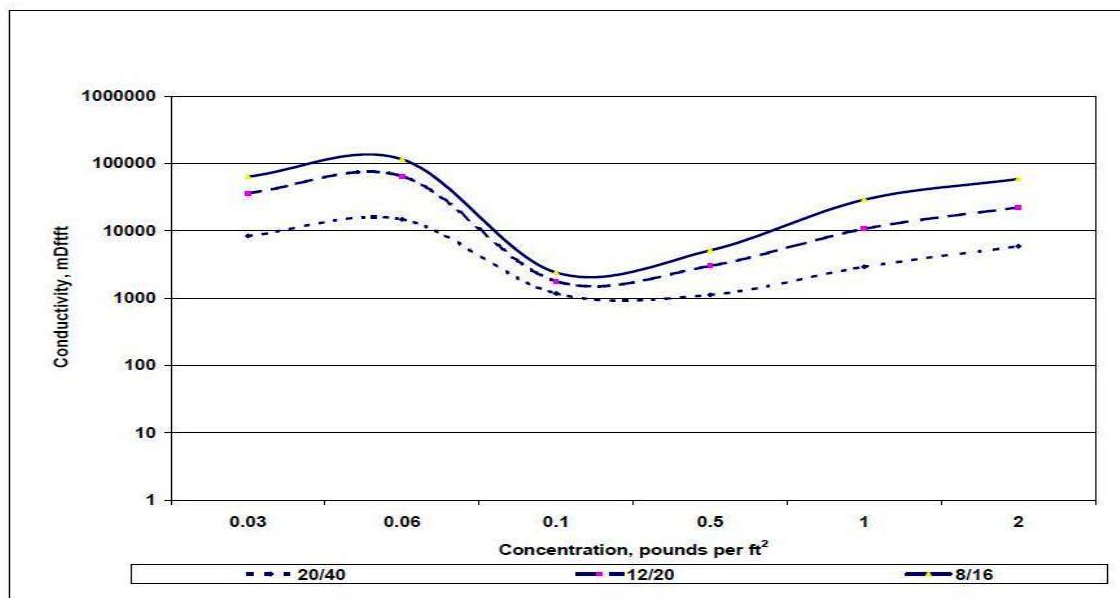


Figure 2.16 Conductivity vs. proppant concentration for various sizes of Brady sand at 1,000 psi closure stress and 100°F

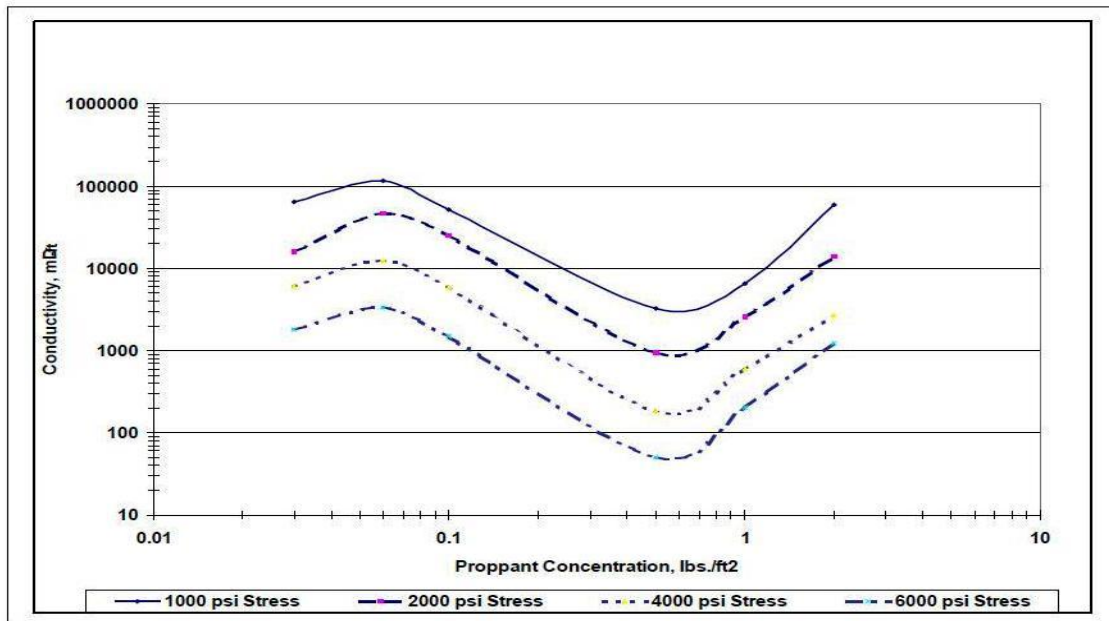


Figure 2.17 Conductivity vs. proppant concentration for 8/12 Brady sand at various closure stress

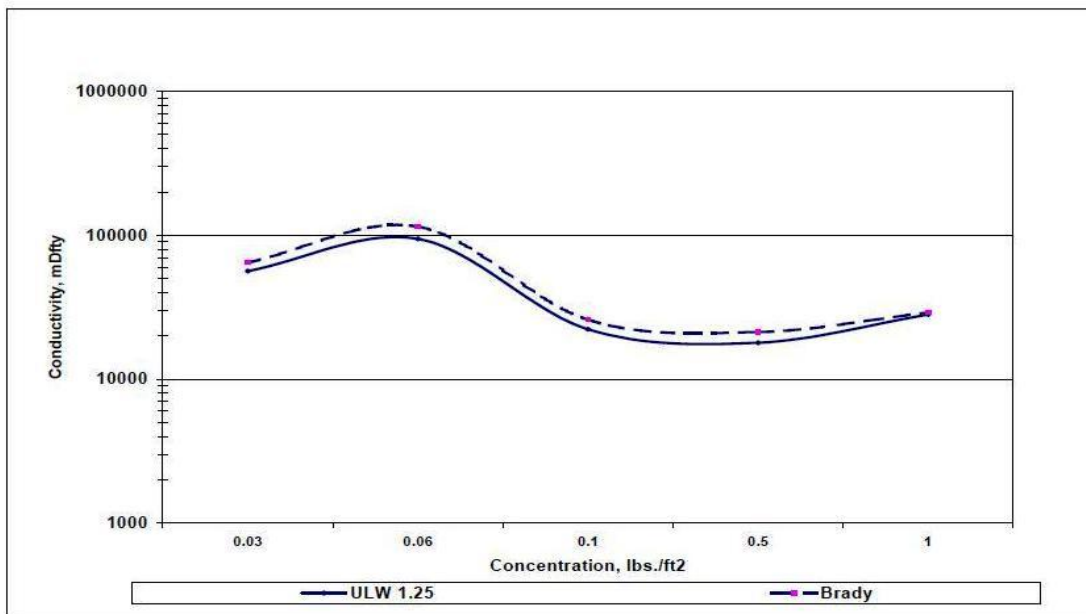


Figure 2.18 Conductivity vs. proppant concentration at 1000 psi closure stress comparing Brady sand and ULW 1.25

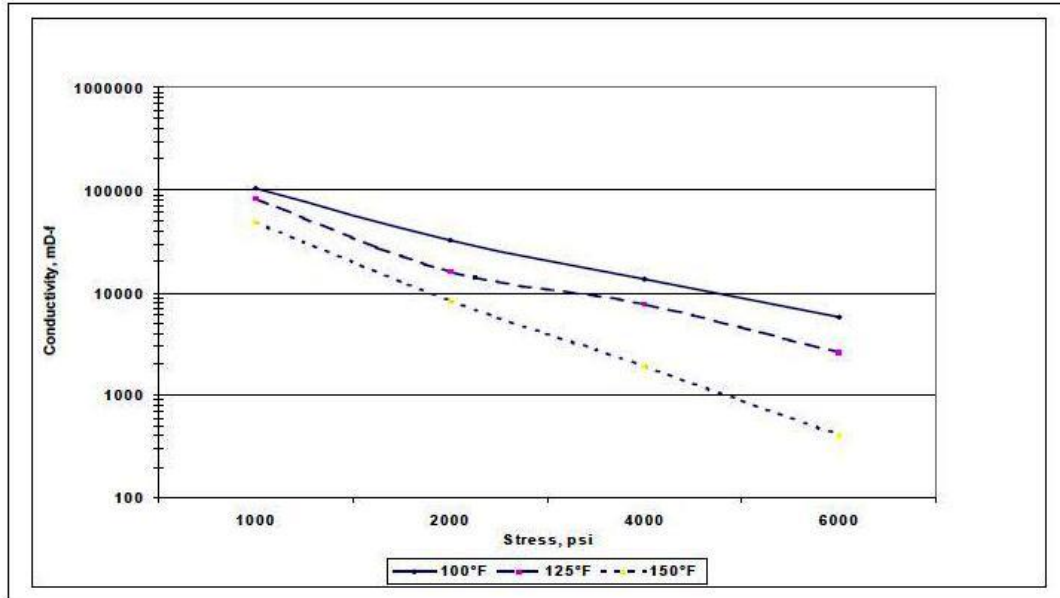


Figure 2.19 Conductivity for 8/12 ULW 1.25 at different confining stress and temperatures

It can be inferred from this study that, increasing the size of proppant enhances the proppant conductivity. Monolayers of both Brady sand and ULW 1.25 were as good as thick packs. Conductivity value of as high as 100000 mD-ft could be achieved using partial monolayers at a closure stress of 1000 psi for these proppants. It should be noted though; sp. gr. of ULW 1.25 is less than half of Brady sand. So, a significantly smaller amount of ULW 1.25 is required to fill the same space as compared to sand particles. As shown in Figure 2.19, increasing temperature decreased the overall conductivity of the ULW 1.25. This decrease was more significant at higher stress levels.

2.2.3. Ultra light weight proppants

As Palisch and Vincent (2008) rightly pointed out, the ideal properties of a proppant for its application in slick water fracturing treatments for low permeability reservoirs would be light as water, high strength, and cheap. But, it is impossible to get all these ideal

properties in one product. Unless, the concept of monolayer can be rightly applied in the field and these individual proppant particles can sustain high stresses for longer periods of time at reservoir conditions. Rickards and Brannon (2004) tested resin coated/impregnated walnut hull proppants and resin coated porous ceramic proppants in their work, where, physical and mechanical properties of these proppants were tested at room temperature. Using Mfrac (Figure 2.20 and Figure 2.21) they tried to highlight better placement properties of light weight proppants with slickwater as compared to sand with slickwater.

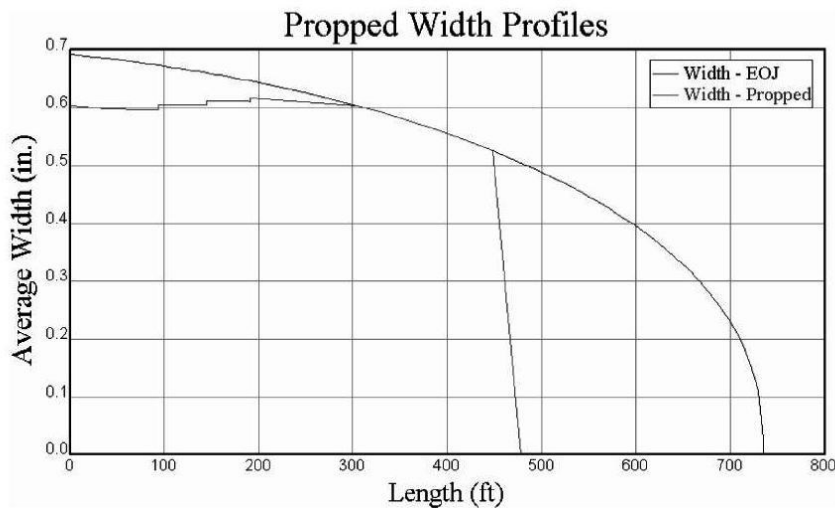


Figure 2.20 Simulation of Ottawa sand proppant placement at pumping rate of 80 bpm using Mfrac simulator

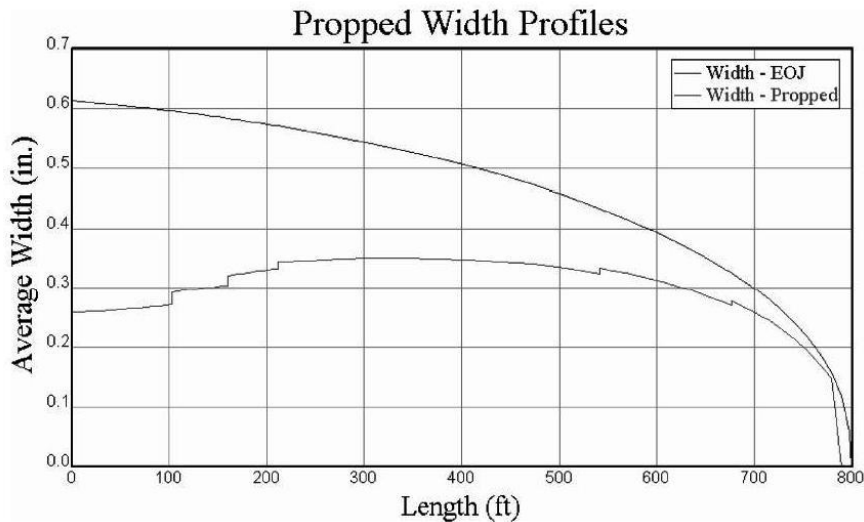


Figure 2.21 Simulation of light weight proppant placement at pumping rate of 80 bpm using Mfrac simulator

Terracina et al. (2010) in their recent publication stressed on the problem of proppant embedment, which is usually overlooked before evaluating proppant performance. While using proppants in soft rocks (soft shales), significant embedment might decrease the conductivity of a monolayer significantly. Though, monolayer of the same proppant might perform very well when used in harder formations (hard shales).

2.2.4. Conclusions

- Slick water fracturing is the stimulation treatment of choice for low permeability reservoirs.
- Settling of conventional proppants is a huge concern in slick water stimulation treatments.
- Partial monolayers of light weight proppants which are easy to transport with slick water might be a solution.
- Crush test might not apply as much to deformable proppants as it does to ceramic proppants and sand grains.

-Application of these proppants has to be shale specific. For example, even after achievement of partial monolayer placement, there might be problems of embedment in softer shales.

-For shales, partial monolayers of deformable proppants might have high enough conductivity.

3. Approach and Methodology

3.1. ESTIMATION OF PHYSICAL PROPERTIES

3.1.1. Bulk Density

The bulk density was evaluated by measuring the volume occupied by pre-weighed proppant sample. This process was repeated three times for each proppant for precision. Precaution was taken so that proppant particles do not stick to the sides of the tube. This could be prevented by pouring the proppants in the cylinder, carefully, using a funnel with a small exit. This bulk density indicates the density measured under no confining stress.

3.1.2. Absolute Density

The measurement of absolute density was done using propyl alcohol as liquid. A fixed amount of liquid and the proppant were brought together and mixed in a vortex (This process makes sure there is no any air bubbles trapped in the proppant pack). The presence of alcohol gets rid of any electrostatic charges present on the sides of the graduated glass tube. Electrostatic charge leads to clinging of particles on the sides of the tube (ISO 13503-2). Proppant particles which are heavier than the liquid settle down. Particles which are lighter stay on the top and the neutrally buoyant ones are dispersed throughout the liquid. Pipette was used to be precise about the amount of liquid which is being used.

3.1.3. Sphericity

Close-up two-dimensional images, with a magnification factor of 23, were taken for randomly selected ten particles of each proppant type. The measurement of sphericity was done in two different ways. Firstly, the close-up images were qualitatively compared to Figure 3.1 and the sphericity and roundness were determined (ISO 13503-2).

Secondly, the definition of Riley's sphericity (Figure 3.2) was used to determine the sphericity of individual particles (Folk). It is to be noted here that for irregularly shaped ULW2 particles, the determination of sphericity and roundness can be highly inaccurate as the image in one plane can look very different from the image in another plane.

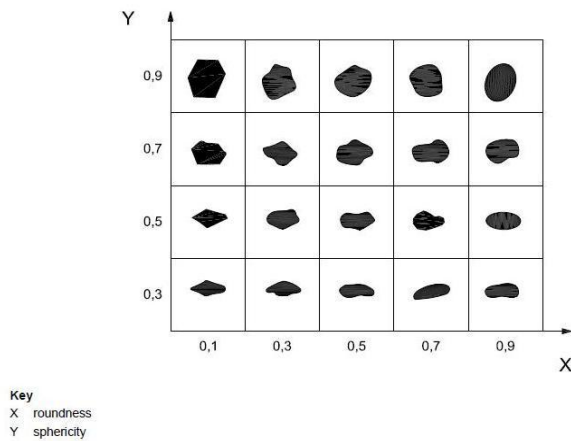


Figure 3.1 Chart for visual estimation of sphericity and roundness, X axis-roundness and Y axis-sphericity

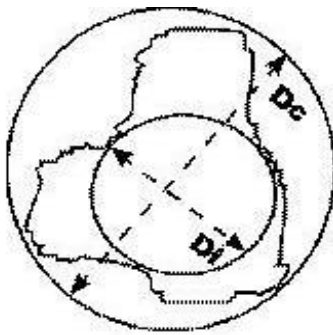


Figure 3.2 Riley Sphericity: $\Psi_R = (D_i/D_c)^{0.5}$

3.1.4. Sieve-size distribution

The sieve size distribution for each type of proppant was done following the guidelines mentioned in ISO 13503-2.

3.2. ESTIMATION OF MECHANICAL PROPERTIES

3.2.1. Strength

The strength of individual particles was tested both at room temperature and higher temperature in a strength test tool fabricated specifically to test individual particles endurance limit. One problem we faced here was for the highly deformable polymeric proppant where we did not see any failure point. The stress range we are interested will be specific to the shale formation in question.

3.2.2. Crush Test

This test was followed by a crush test just to highlight the point that ULW1 and ULW2 do not form as much fines as ULW3 does. Here failure point of the proppant pack as a whole does not matter as much as the amount of fines generated as a result of crushing. The crush test was performed at two different temperatures, ~25°C and ~95°C. The crush test was done at a stress level of not more than 15000 psi. Stress was held at specified stress level for two minutes. The end product of the crush test was screened through appropriate sieve to see how much proppant was crushed into comparatively finer particles.

3.2.3. Conductivity Test

The results of conductivity tests under varied conditions are most important before making a selection of proppants for any fracturing job. The long term conductivity tests were performed following guidelines specified in ISO 13503-5. All the conductivity tests were done at ~95°C with pure DI water as the fluid of choice which has a viscosity of 0.316 cP at ~95°C. The back pressure was maintained at 400 psi which lies in the range (300 psi-500 psi) specified in ISO 13503-5.

4. Description and Application of Equipment and Processes

4.1. ESTIMATION OF PHYSICAL PROPERTIES

4.1.1. Bulk Density

As shown in the Figures 4.1, 4.2 and 4.3, a certain weight of proppant was taken and placed in a graduated glass cylinder and its bulk volume was evaluated. This process was repeated three times for each proppant. A good repeatability and a good comparison with results from other sources (Rickards and Brannon, 2003) confirmed our method was quite accurate. It should be pointed out here that ULW-1 in particular had a tendency of sticking to the walls of the cylinder. This could be prevented by pouring the proppants in the cylinder, carefully, using a funnel with a small exit, so that particles do not stick to the walls of the cylinder.



Figure 4.1 Bulk density measurement for ULW 1 in a graduated glass cylinder



Figure 4.2 Bulk density measurement for ULW 2 in a graduated glass cylinder



Figure 4.3 Bulk density measurement for ULW 3 in a graduated glass cylinder

4.1.2. Absolute Density

To measure the absolute density, a certain weight of proppant was added to 4 ml of propyl alcohol and allowed to settle down. The mixture was placed on a vortex to mix it well and get rid of any trapped air bubbles. Therefore the absolute volume of the solid proppants was calculated and used in evaluation of absolute density of proppant particles. Figures 4.4, 4.5 and 4.6 show how proppant particles were well settled in propyl alcohol during the study. It can be noticed in the same figure that, in case of ULW1, some proppant particles are floating on the top, while a few others remain neutrally buoyant, which indicates; there is a variation in absolute density among various proppant particles.



Figure 4.4 Absolute density measurement for ULW 1 in a graduated glass cylinder using propyl alcohol



Figure 4.5 Absolute density measurement for ULW 2 in a graduated glass cylinder using propyl alcohol



Figure 4.6 Absolute density measurement for ULW 3 in a graduated glass cylinder using propyl alcohol

4.1.3. Strength and Crush Test

The equipment shown in Figure 4.7 was used for evaluating the strength of individual proppant particles. The equipment has three parts, top piston, bottom piston and cylindrical sleeve. The whole equipment is made out of aluminum to keep the tool light in weight, but, the surfaces of the pistons which are in contact with the proppant particle are made out of tool steel, so that proppant does not embed into the equipment during the test. The equipment is placed in a Humboldt press machine. It is to be noted here that the whole set-up is designed in a way that strain is controlled by the interface of the machine which results in stress.

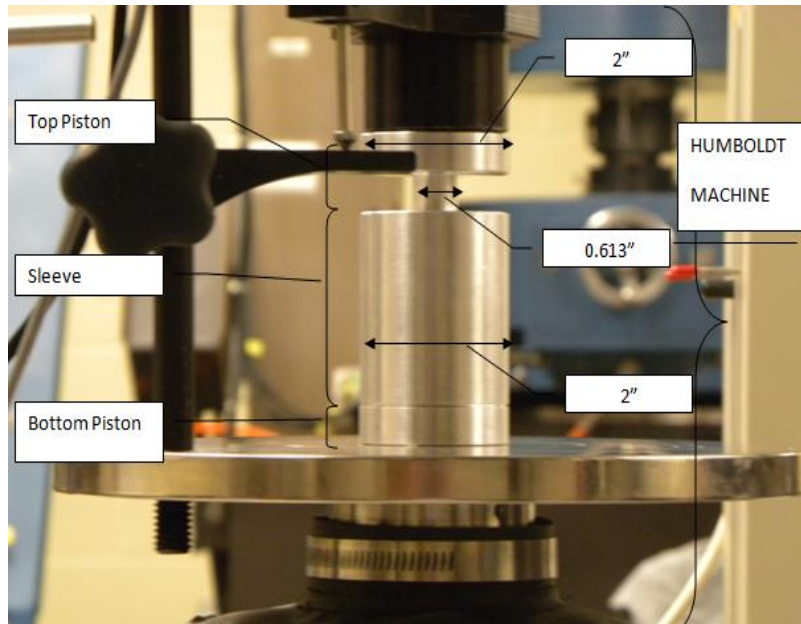


Figure 4.7 Tool used for testing strength of proppant in a HUMBOLDT strength test machine

The crush test is not so significant for ULW1 and ULW2, as they are not expected to form fines due to their deformable nature. The ULW3, a ceramic proppant, is expected to form significant amount of fine formation on application of higher stress.

4.1.4. Conductivity Test

API conductivity cell was used to evaluate long term proppant pack conductivity at four different stresses (1000 psi, 2000 psi, 4000 psi and 6000 psi) at the Barnett shale temperature of around 95 degrees centigrade. Figure 4.8 shows the API cell in the press inside an oven. The concentration was varied from 0.03 lbm/ft² (sparse partial monolayer) to 1 lbm/ft² (thick proppant pack) (Brannon and Malone, 2004). Figure 4.8 indicates the flow experiment set-up we used, which includes an API cell on which the stress was applied using a load press. Using an average value for diameter of the particle in the proppant pack, a Reynolds number was calculated. This number was kept below 10 to stay in the Darcy regime (Bird and Stewart). This implied the flow-rate never exceeded 20 ml/min. The pulsation of pump was dampened by using accumulators to store the flowing fluid (DI water) (ISO 13503-5). The whole set-up (API cell and accumulator) was kept inside an oven maintained at 95°C (Barnett shale temperature). The flow rate of the effluent was recorded to check if it matches with the flow rate controlled by the pump. A good match indicates absence of any leak. The pressure was recorded through pressure ports through two separate differential pressure transducers connected in parallel to each other. The pressure of the proppant pack was recorded through a central pressure port.

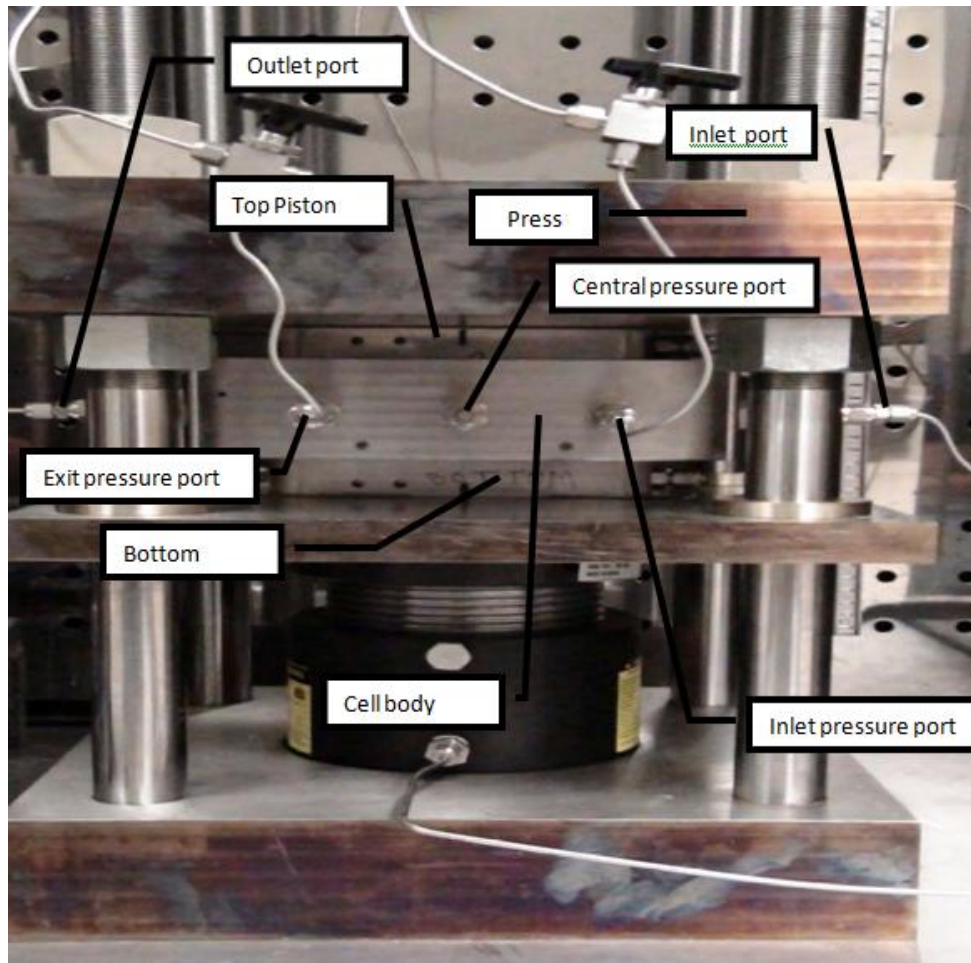


Figure 4.8 API conductivity Cell under stress inside an oven maintained at 95°C

Leak in the system was the major problem in our set-up. The O-rings in the top and bottom piston were not enough to provide a leak proof seal. Rubber sheets (0.1" thick) cut in the shape of the metal shims were used in between the top piston and top metal shim and in between bottom metal shim and the bottom piston. On application of any stress the rubber sheets provided a very good seal.

The width of the pack at various stresses was calculated according to the guidelines outlined in ISO 13503-5. The ports for inlet, outlet and pressure measurement were made smaller by use of threaded screws whose inner end were leveled with the

inside of the API cell. This was done specifically for testing the monolayer and the other proppant packs whose thickness was smaller than the diameter of the ports. These experiments are oriented towards application of these proppants in Barnett Shale. These shales are harder and embedment is not a problem. So, use of metal shims instead of the Barnett shale core in our experiment is justifiable. But, if these proppants are intended to be used in softer shales, like Haynesville, replacing metal shims with actual cores will be appropriate.

5. Results

5.1. ABSOLUTE DENSITY, BULK DENSITY, POROSITY AND SPHERICITY

Table 5.1 shows the results for measurement for absolute density, bulk density, bulk porosity and sphericity.

	ULW1	ULW2	ULW3
Specific Gravity	0.95	1.25	2.3
Density of Pack (g/cc) (without closure stress)	0.6	0.77	1.19
Porosity of Pack (without closure stress)	44 %	36 %	31%
Sphericity	1	0.62±0.7	0.78±0.1

Table 5.1 Tabular representation of bulk density, nominal density, porosity and sphericity for the three proppants being studied

Specific gravity indicates the actual density of the proppant particles. Isopropyl alcohol (sp. gr. = 0.781 gm/ml) was used for evaluation of specific gravity. Most of the particles for each of the proppants settled down in propyl alcohol during the evaluation of absolute density. Bulk density is the weight of 1ml of proppant. Ottawa sand has a sp. gr. of 2.65 and a bulk density of 1.65 gm/ml. The idea of using these proppants is to use smaller mass of proppants occupying the same volume as would a larger mass of the conventional proppant, like, Ottawa sand. Porosity calculation results directly from the bulk density measurement. The values for sphericity in Table 5.1 indicate Riley's sphericity values. A value of one indicates well roundedness and a smaller value indicates

presence of angularity. As indicated in Table 5.1 and Figures 5.1, 5.2 and 5.3, ULW1 is completely spherical, ULW2 is extremely angular and ULW3 is intermediately spherical.

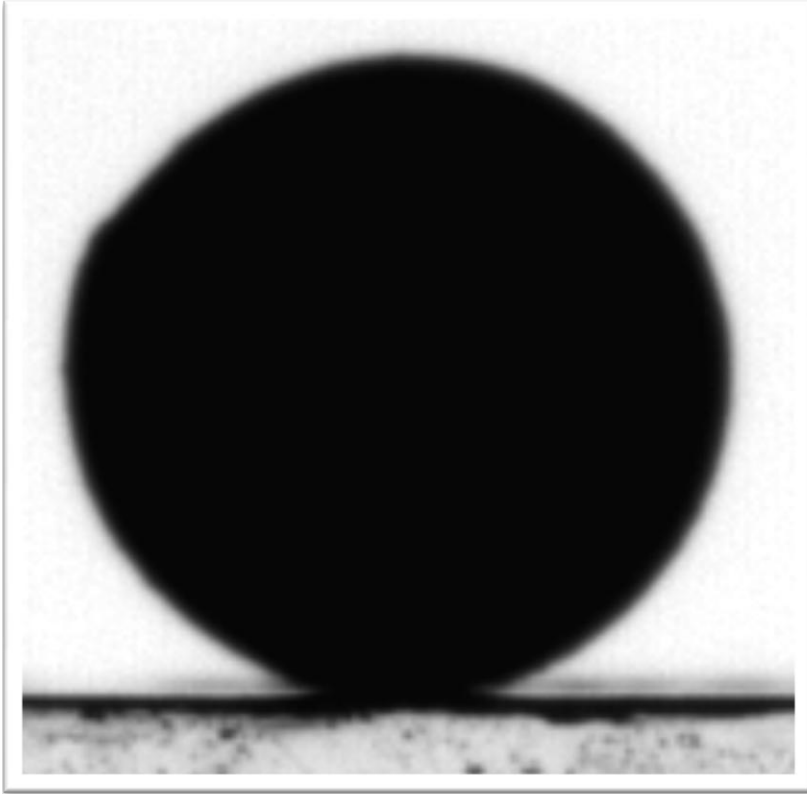


Figure 5.1 Two-dimensional close up image of ULW 1

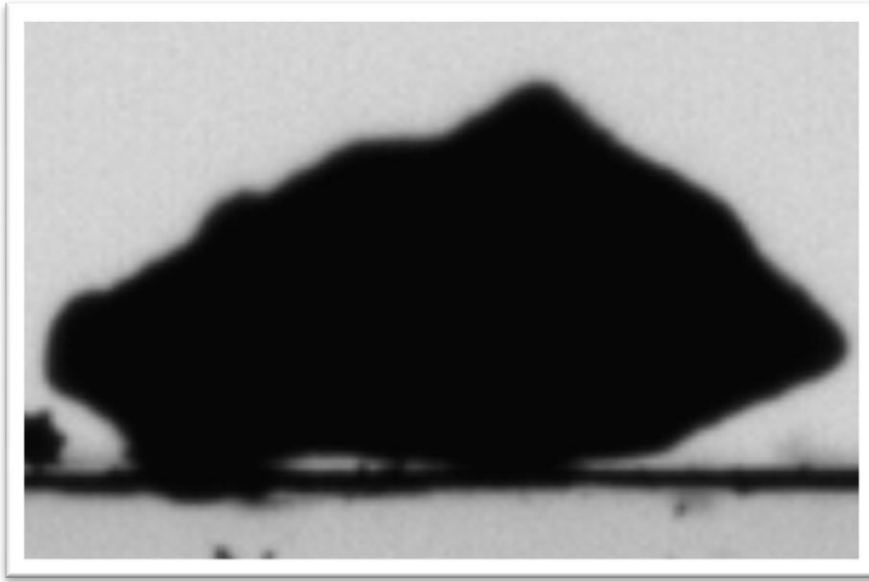


Figure 5.2 Two-dimensional close up image of ULW 2

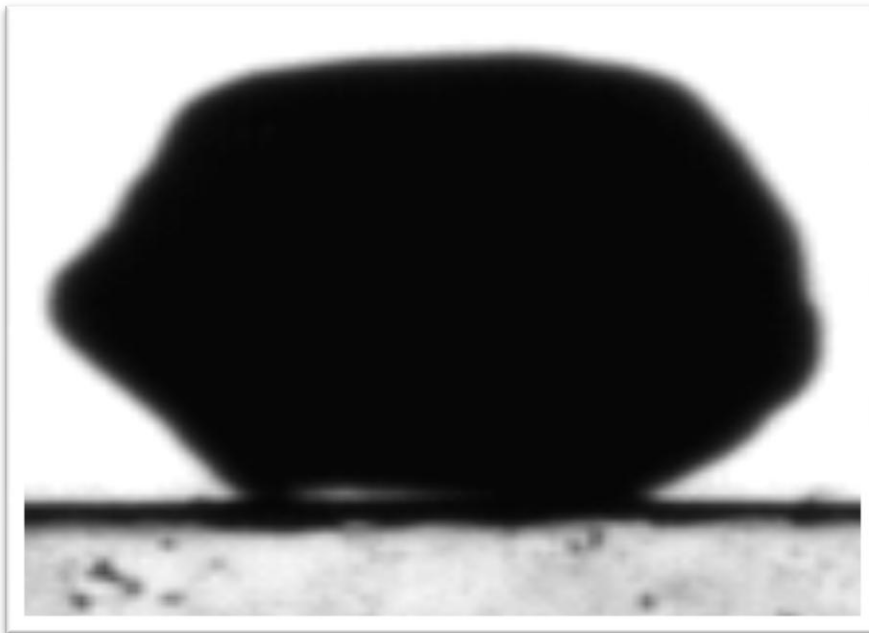


Figure 5.3 Two-dimensional close up image of ULW 3

ISO 13503-2 characterizes the shape of proppants in terms of sphericity and roundness, both of which vary from 0 to 1 (where 1 stands for perfectly round and spherical). Figure 5.4 clearly shows the sphericity and roundness values for ten randomly selected particles for each kind of proppant.

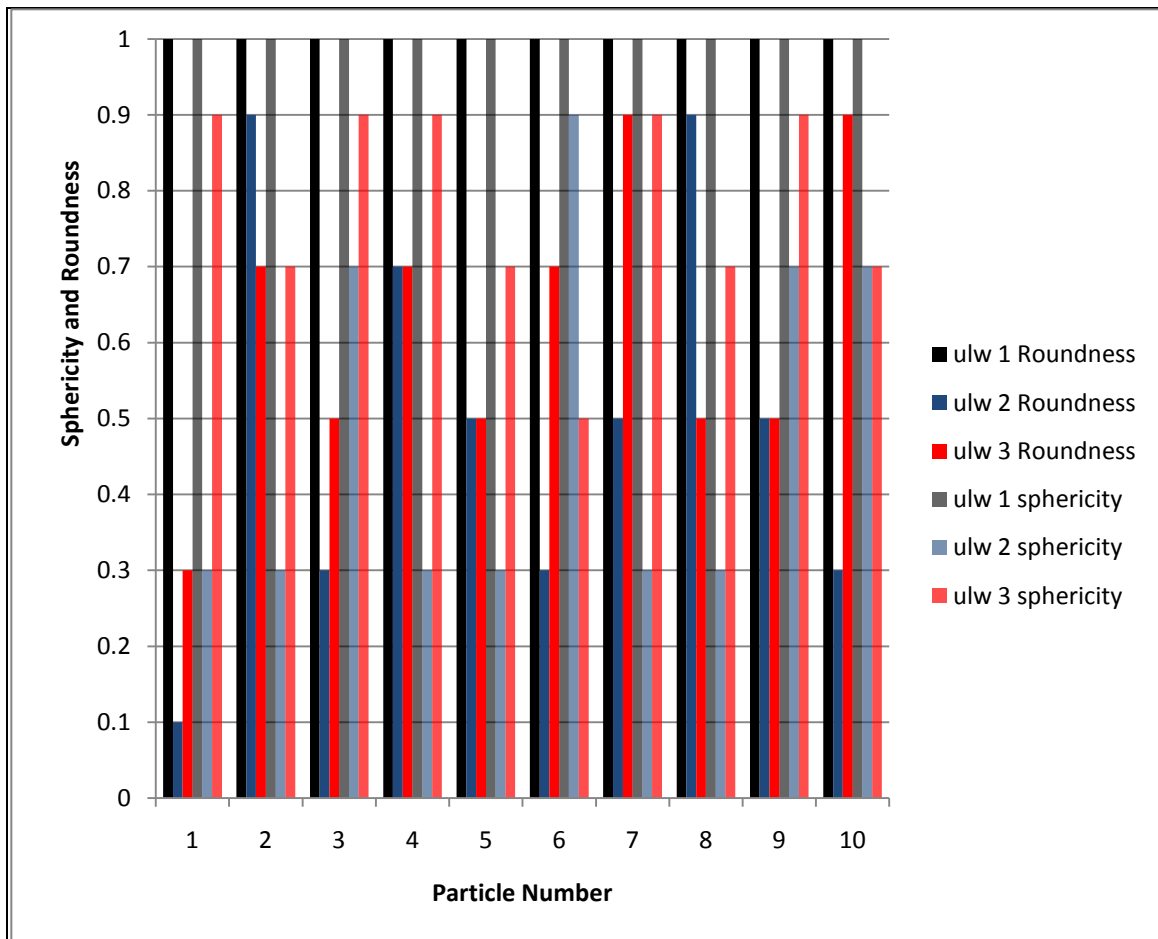


Figure 5.4 Sphericity and Roundness distribution for three types of proppants ULW 1, ULW 2 and ULW 3

ULW1 is a perfect sphere. ULW2 has smallest values for sphericity and roundness. ULW3 is intermediately round and spherical.

5.2. SIZE DISTRIBUTION

Figure 5.5 shows the sieve size distribution. Sieve size analysis was done on 80 grams of each proppant type following the guidelines of ISO 13503-2. ULW2 due to its angularity has a wider distribution than ULW1 and ULW3.

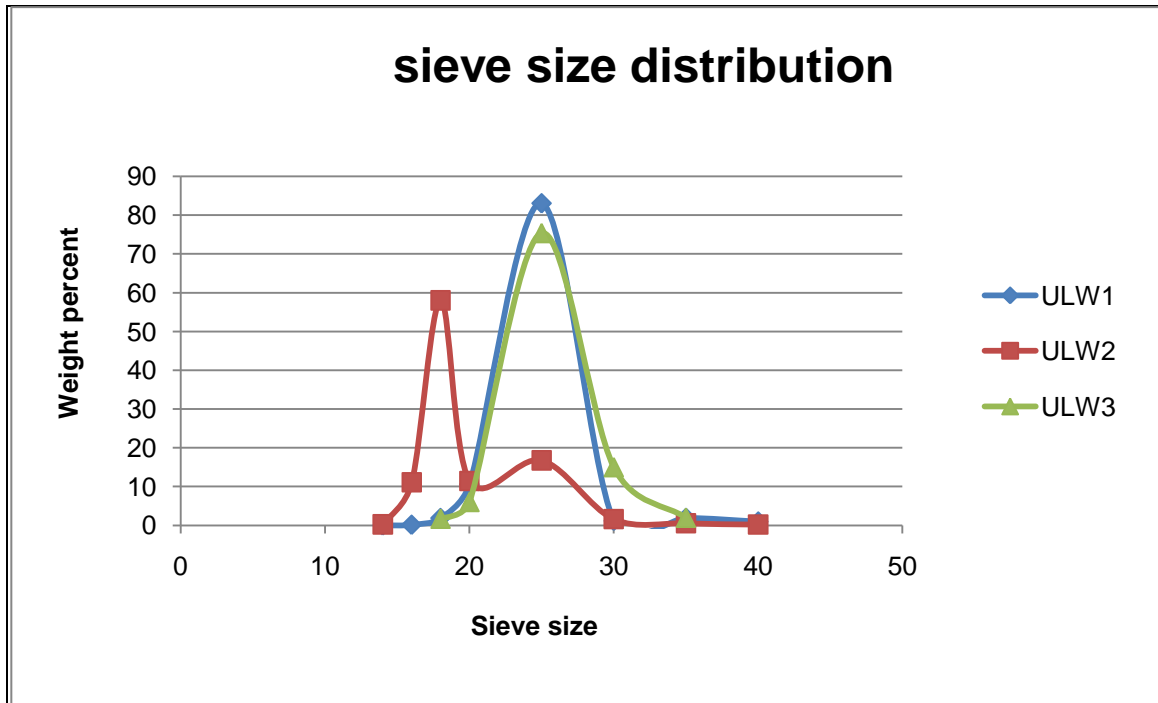


Figure 5.5 Size Distribution of the three types of proppants

5.3. CRUSH TEST

Following the guidelines stated in ISO 13503-2, the crush test was done on each type of proppant to a stress level of up to 15000 psi at room temperature. ULW1, due to its deformable nature formed very small amount of fines. The amount of fines formed never exceeded 5% by weight. The same concept applies to ULW2, in which the amount of fines formed never exceeded 3% by weight. But, for ULW3, almost 14% of original amount resulted in fines formation. It will be shown in the results of conductivity tests

later, that, while using ultra-light weight proppants, a partial monolayer between fracture faces can provide reasonable conductivity. So, fine formation for a partial monolayer may not be a huge problem. For a thick proppant pack on the other hand fine formation will definitely result in loss of permeability of the pack. Another concern with fine formation is plugging of pore space in an already less permeable shale formation. It should be noted that stress levels in shale formations vary according to the depth and the stress gradient. As shown in Figure 5.6, the maximum stress which the proppants might have to endure is in Haynesville does not exceed a value of 7000 psi. The point to be noted here is, stress level at which the crush test is done at, does not imply a stress of 15000 psi can be reached in any of the shale formations. The crush test is designed to compare the crush behavior of various proppants at the same level of stress. The stress levels shown in Figure 5.6 are values for effective horizontal stress which is calculated using the following equations.

The absolute vertical stress, σ_v is given by

$$\sigma_v = (1.1 \text{ psi/ft}) h, \text{ where 'h' is the depth in feet,} \quad (5.1)$$

The effective vertical stress, σ_v' is given by

$$\sigma_v' = \sigma_v - \alpha p, \quad (5.2)$$

where α is Biot's poroelastic constant and has a value of 0.7 for hydrocarbon bearing formations (Economides and Hill) and p is the pore pressure. The effective minimum horizontal stress, σ_H' is given by

$$\sigma_H' = (v / (1-v)) \sigma_v', \quad (5.3)$$

where v is the Poisson's ratio, and has been assigned an average value of 0.3 for this study. This value might be different for different formations. Maximum possible value for minimum horizontal stress, which the proppants are expected to endure when the reservoir is, depleted i.e. $p=0$, has been used in this study. Figure 5.6 also supports the idea that "No two shale gas plays are alike" (Halliburton – Shale). The same test was done at a Barnett shale temperature of around 95 degrees centigrade. The amount of fines formed for ULW1 was less than 0.6% this time. For ULW2 fine formation was less than 2% in all cases. This indicates with increase in temperature ULW1 and ULW2 tend to become more deformable and form even lesser amount of fines. For ULW3, an increase in temperature increased the brittle behavior of the proppants and amount of fines formed was around 30% of original weight, as compared to 14% loss at room temperature.

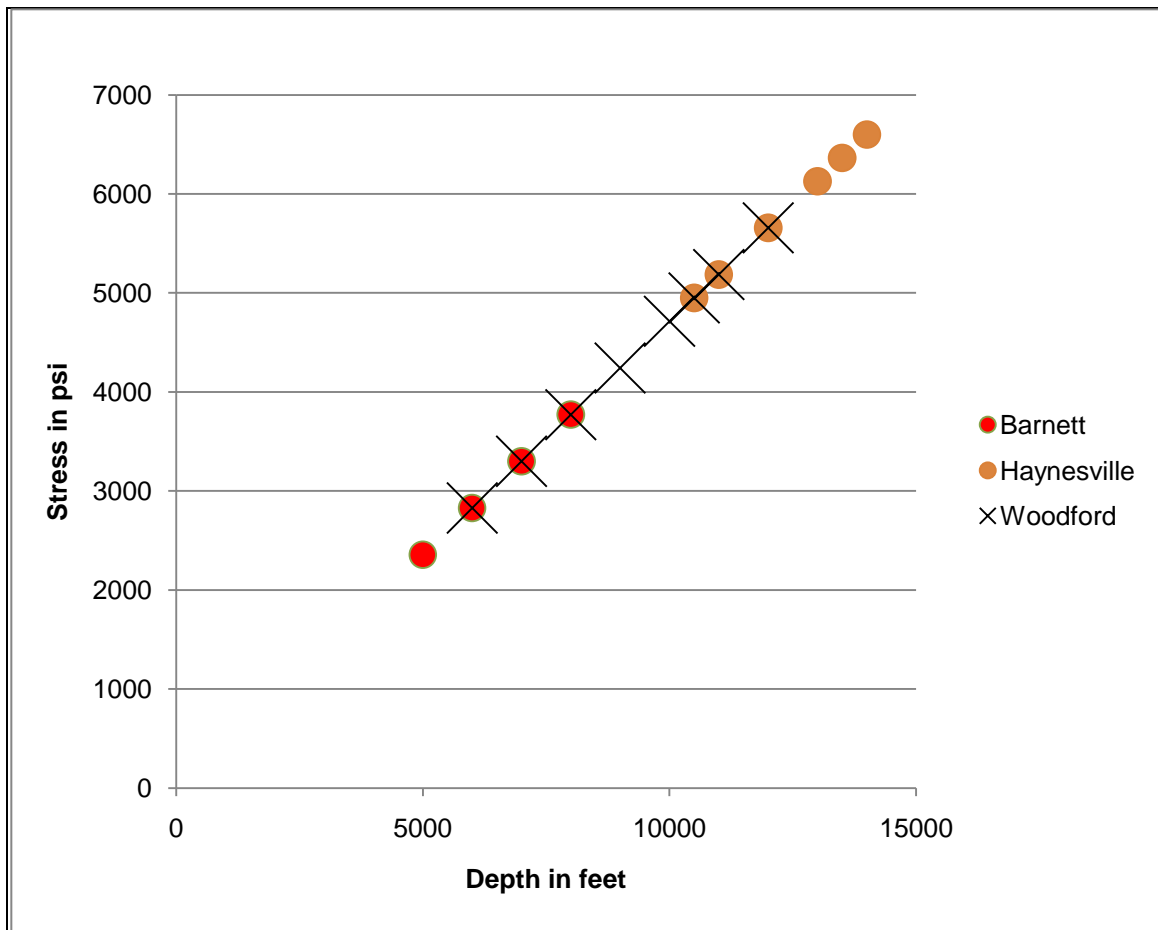


Figure 5.6 Maximum possible values for horizontal stresses in Barnett shale, Haynesville shale and Woodford shale

An average value of Young's Modulus was also calculated for each case using the slope of the stress-strain curve. Figures 5.7-5.12 show the plots for stress-strain curve for each case. Table 5.2 indicates weight loss due to fine formation and also the Young's Modulus for each case.

	Stress=15000psi @ room temperature % fines formed	Stress=15000psi@ 95 degrees % fines formed	Stress=15000psi @ room temperature Young's Modulus	Stress=15000psi@ 95 degrees Young's Modulus
ULW1	~4% by weight	~0.5% by weight	25000 psi	20000 psi
ULW2	~1.4% by weight	~1.5% by weight	25000 psi	20000 psi
ULW3	~14% by weight	~30% by weight	45000 psi	45000 psi

Table 5.2 Tabular representation of fines formation and Young's modulus value for proppant packs for various cases

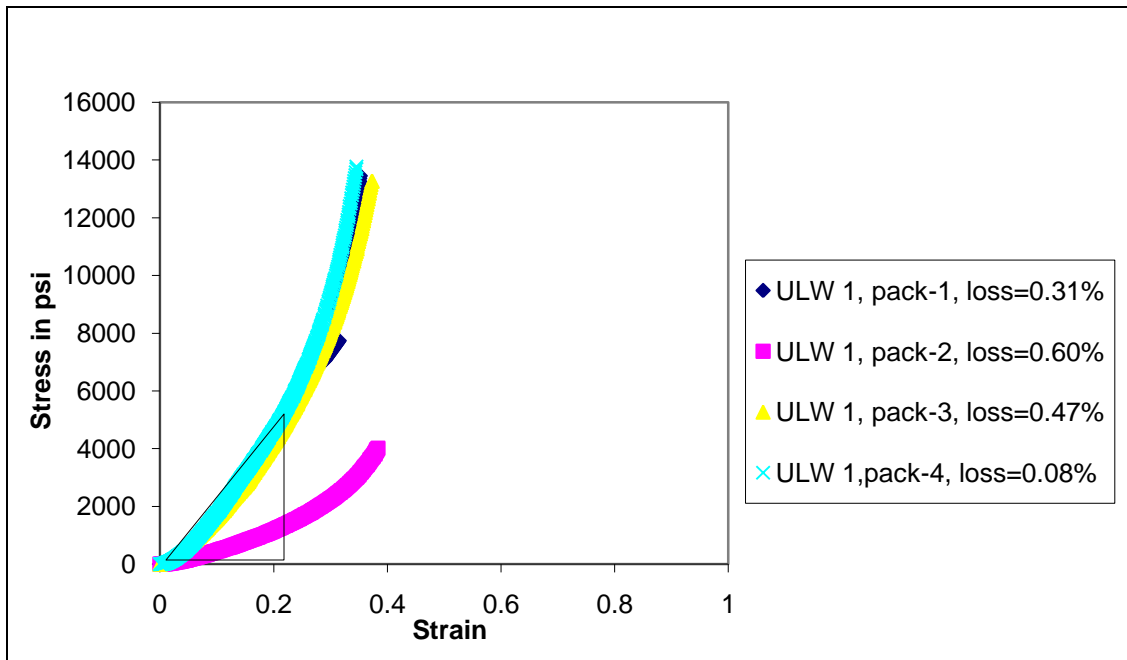


Figure 5.7 Stress vs. Strain curve for ULW 1 at ~95°C

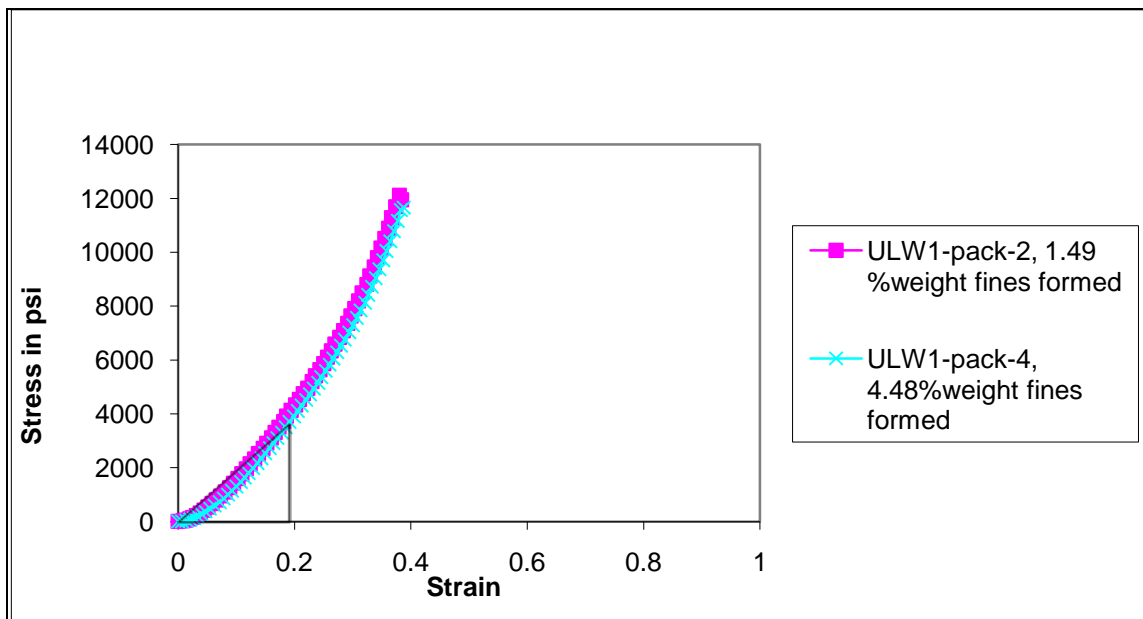


Figure 5.8 Stress vs. Strain curve for ULW 1 at ~25°C

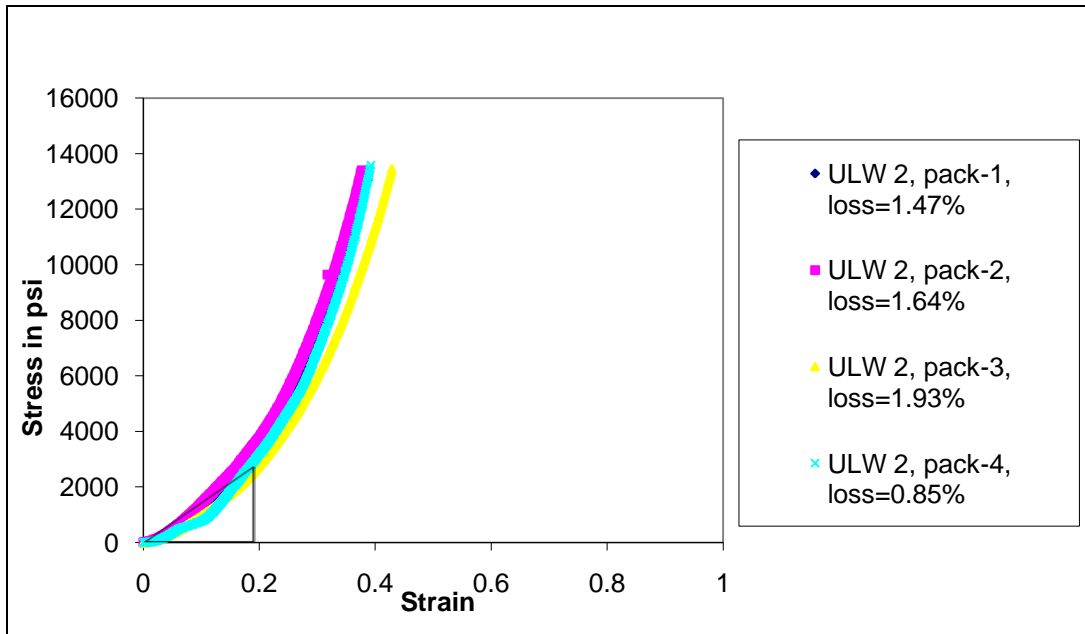


Figure 5.9 Stress vs. Strain curve for ULW 2 at ~95°C

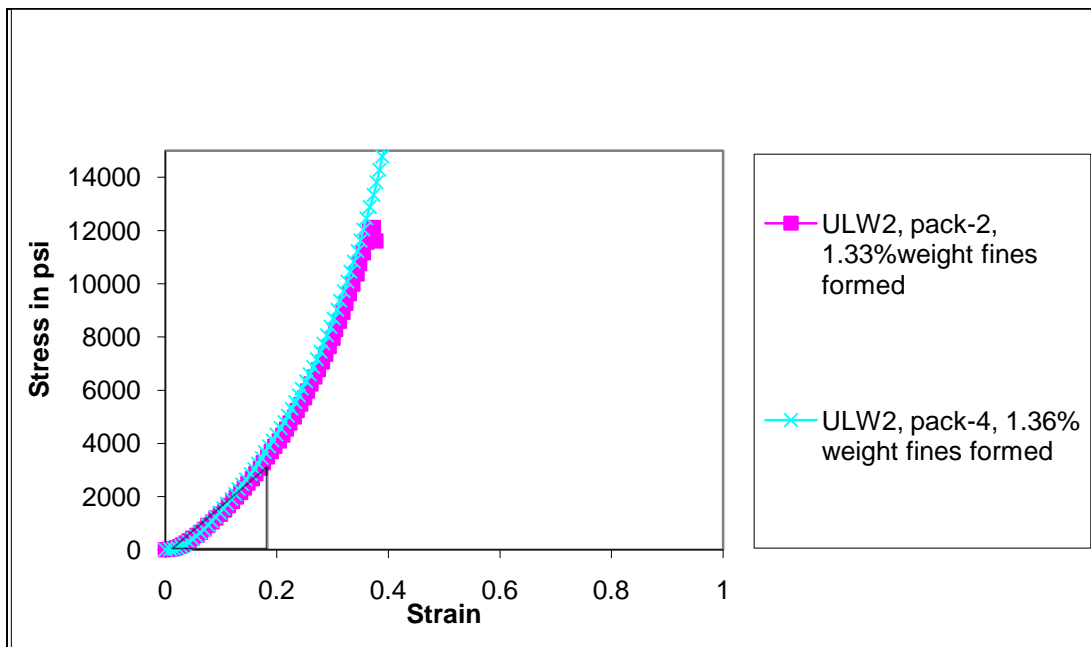


Figure 5.10 Stress vs. Strain curve for ULW 2 at ~25°C

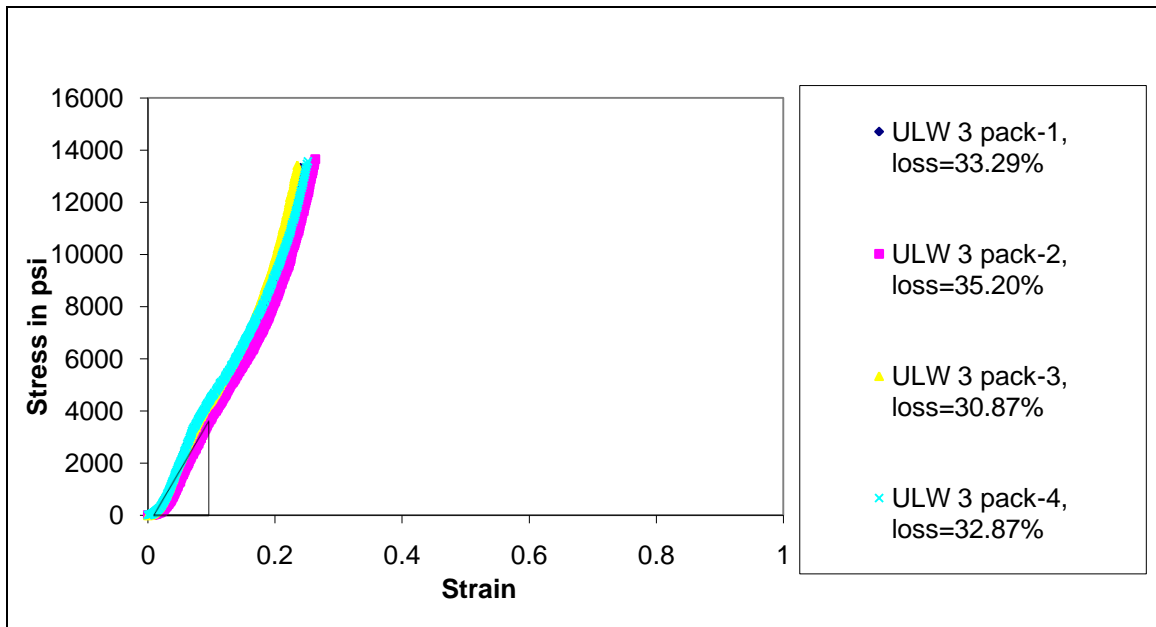


Figure 5.11 Stress vs. Strain curve for ULW 3 at ~95°C

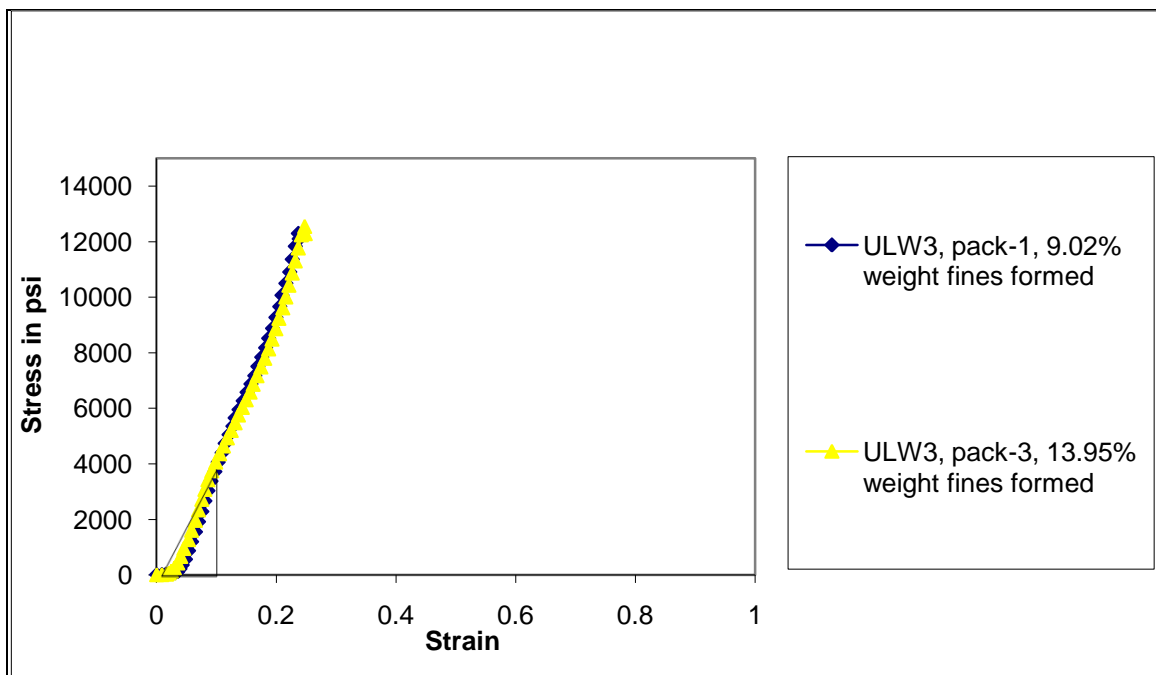


Figure 5.12 Stress vs. Strain curve for ULW 3 at ~25°C

5.4. STRENGTH TEST OF SINGLE PROPPANT PARTICLE

After the strength test of the pack, strength of individual proppant particles was evaluated to examine the variation among the proppants. The mechanical behavior was tested at both room temperature and Barnett shale temperature (~95° C) to assess the change in behavior of proppants with the increase in temperature and also to determine the applicability of the proppants in Barnett shale.

5.4.1. ULW 1

Figure 5.13 shows the applied load and the resulting deformation for 5 single ULW1 particles tested at 95 °C. Particles 1, 3-5 do not show definite failure points. Particle 2 fails at 27 lbf. Figure 5.14 shows the applied load and the resulting deformation for 10 single particles tested at the room temperature. The load at failure is lower at the room temperature compared to that at 95 °C. These proppants can withstand the stress without getting crushed. This is due to the deformable nature of this polymeric proppant. Of course, these proppants deform under stress and reduce the fracture conductivity. Fracture conductivity would be studied in the next task where the applicability of the proppant has been determined.

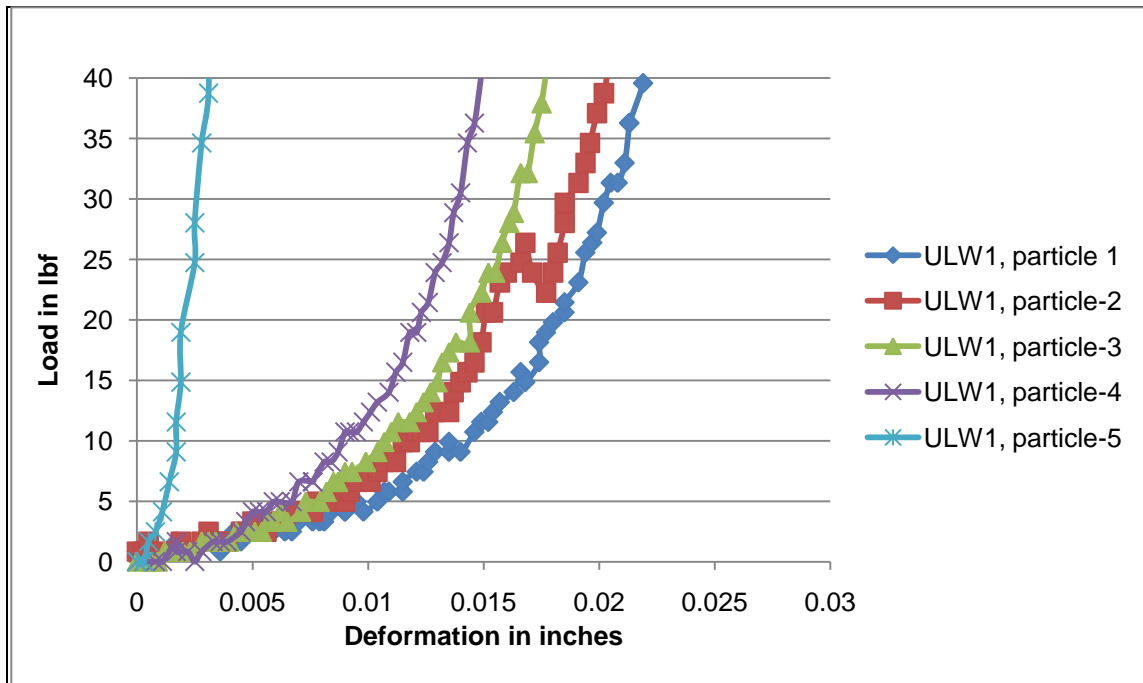


Figure 5.13 Strength test for single particles of ULW 1 at ~95°C

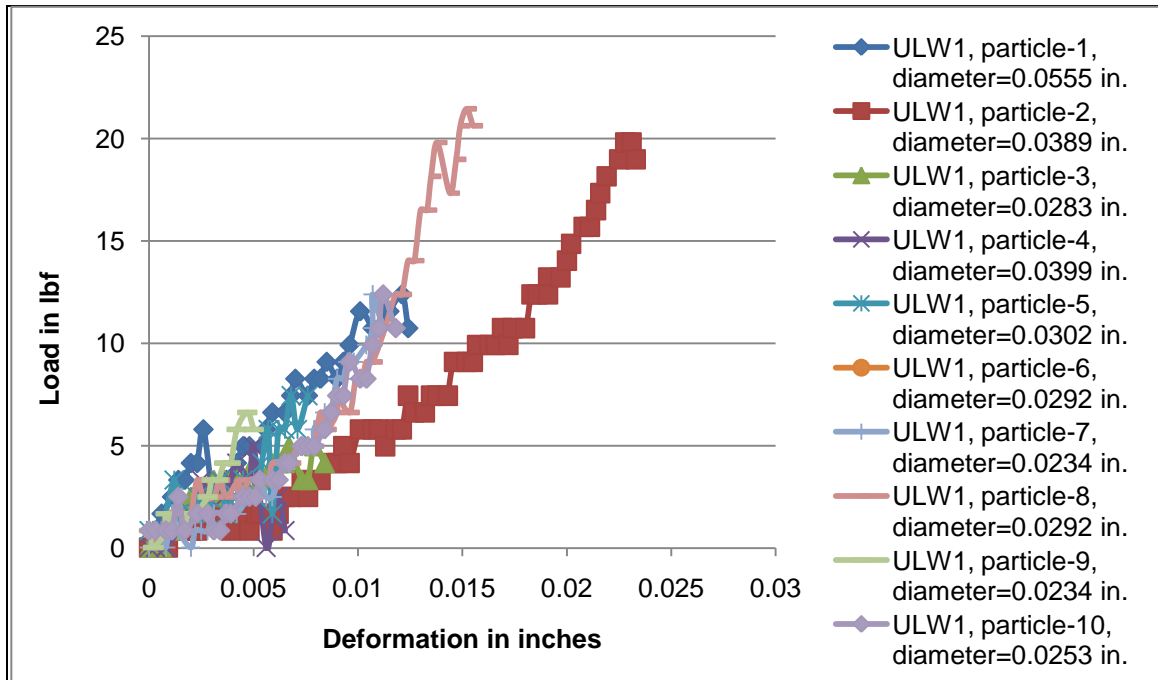


Figure 5.14 Strength test for single particles of ULW 1 at ~25°C

5.4.2. ULW 2

Figs. 5.15 and 5.16 show the applied load and the resulting deformation for 5 single ULW2 particles tested at $\sim 95^\circ\text{C}$ and room temperature, respectively. At the higher temperature, the curves seemed to have stretched, i.e., deformations are larger for the same load applied, indicating increase in elasticity of the proppants with increasing temperature.

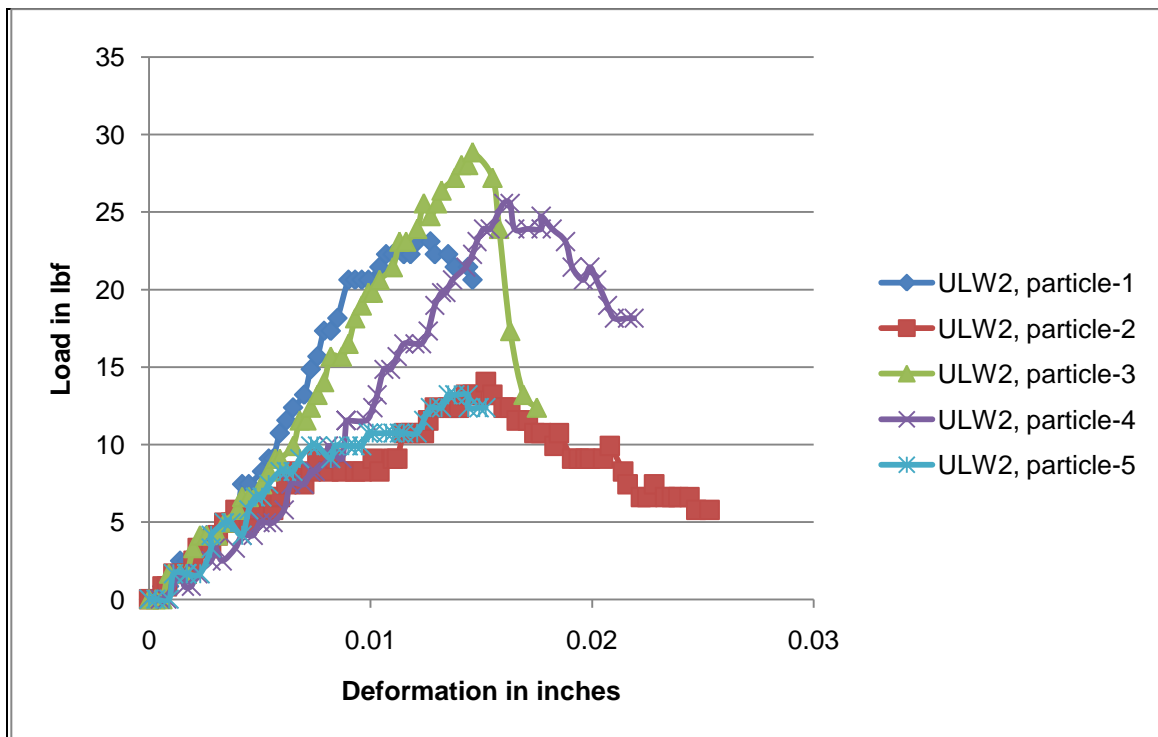


Figure 5.15 Strength test for single particles of ULW 2 at $\sim 95^\circ\text{C}$

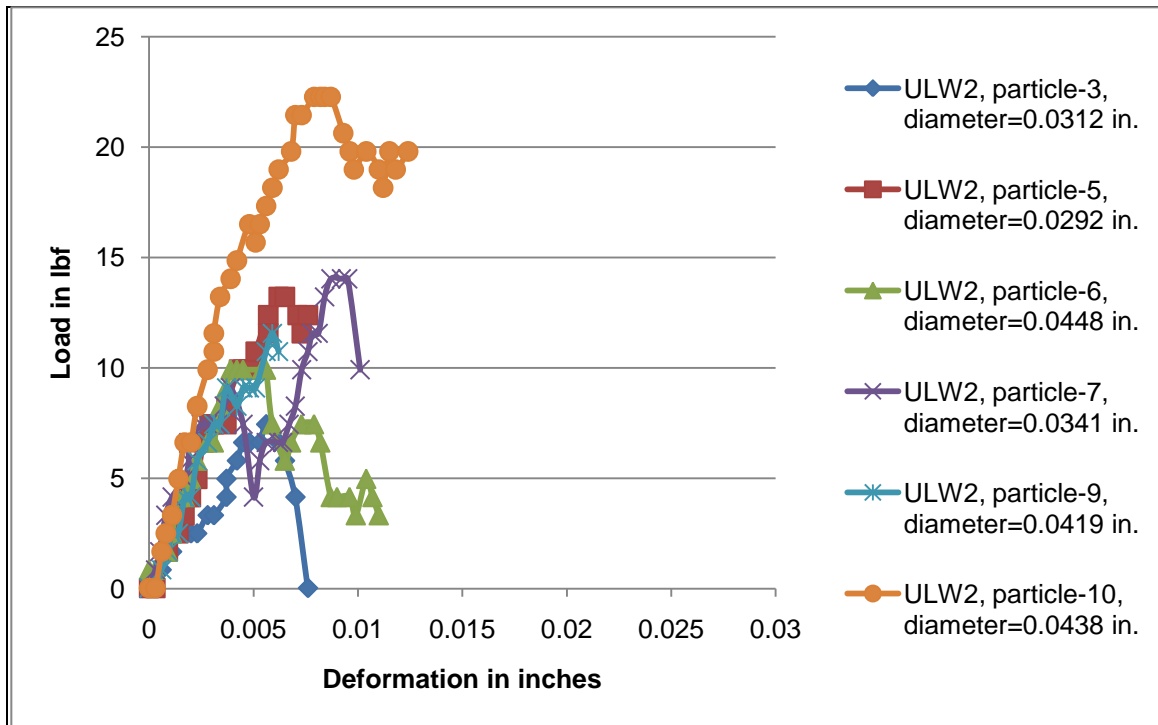


Figure 5.16 Strength test for single particles of ULW 2 at ~25°C

5.4.3. ULW 3

Figs. 5.17-5.18 show the applied stress and the resulting strain for 5 single ULW3 particles tested at ~95 °C and room temperature, respectively. The deformations at which individual particles fail are very low compared to those of the previous two proppants, indicating the brittle nature of ULW3, a ceramic proppant.

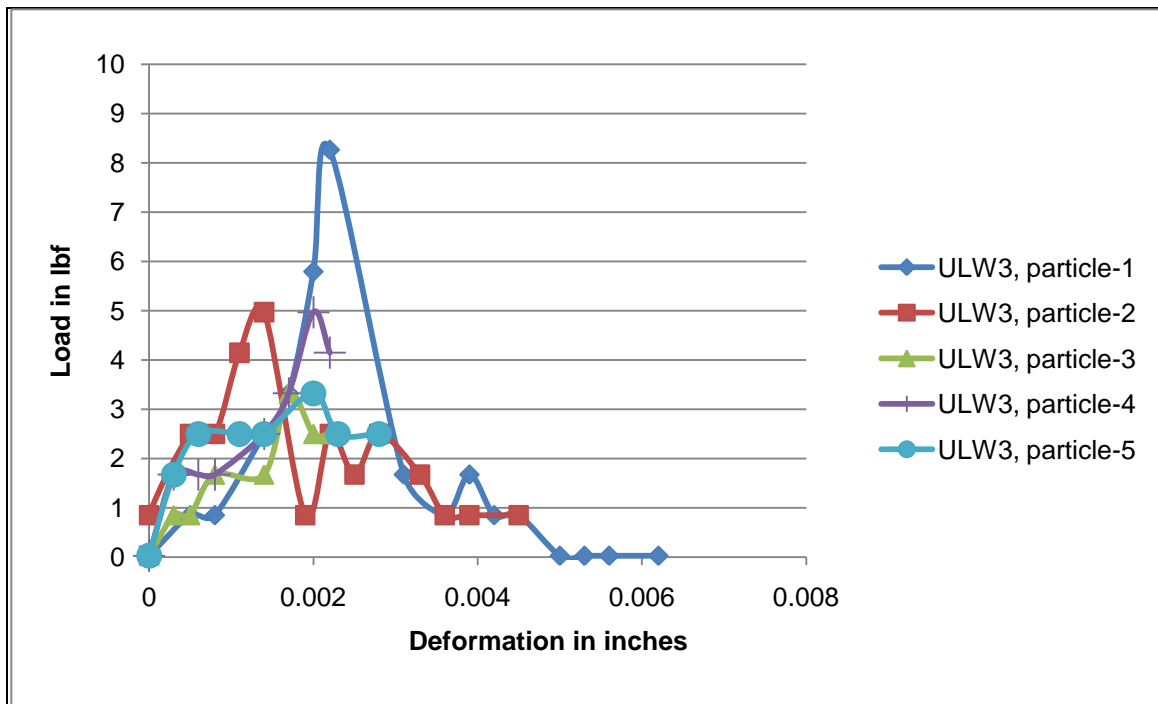


Figure 5.17 Strength test for single particles of ULW 3 at ~95°C

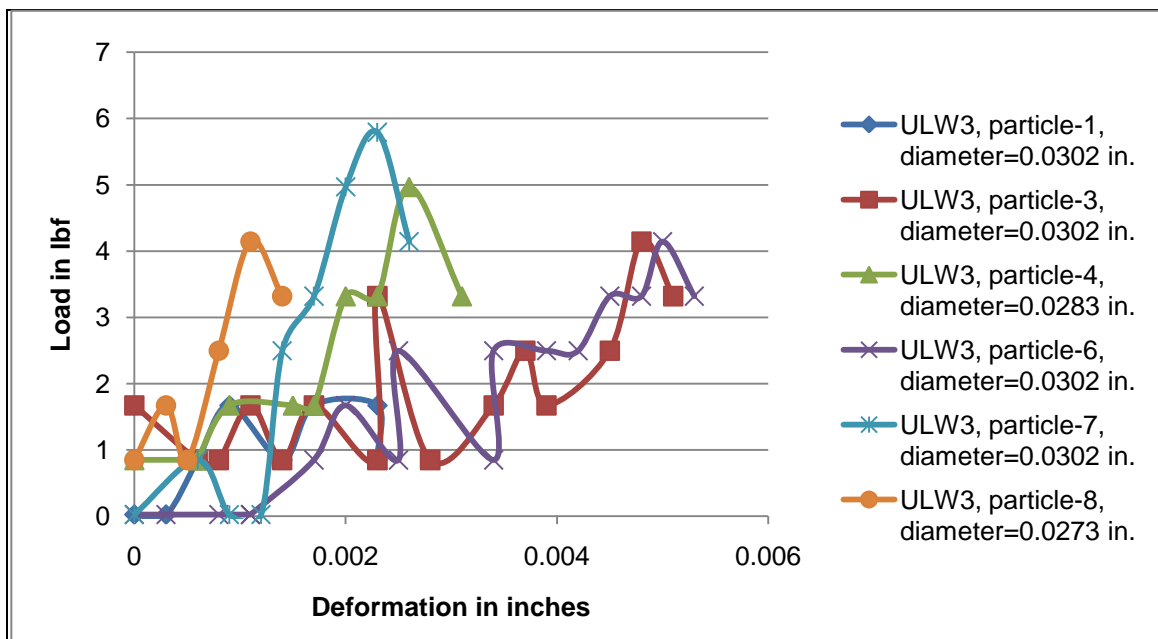


Figure 5.18 Strength test for single particles of ULW 3 at ~25°C

5.5. DEFORMABILITY

The load-deformation data for individual proppants have been converted to “effective stress” versus “effective strain” plots (Figures 5.19-5.21). The values of stress and strain have been calculated on the basis of the initial dimension of the particle. It is an effective value because the particles deform and the distribution of stress is not uniform on round or irregularly shaped particles. It is to be noted that the strain scale in all the three plots is kept constant to show the elasticity of proppants with respect to each other. A higher slope (or higher value of Young’s modulus) indicates less deformability.

Figure 5.19 shows that ULW1 is the most deformable. Many particles deform beyond an effective strain of 0.5 without failing. The Young’s modulus varies significantly between particles. The largest particle had the highest Young’s modulus in this sample. ULW2 is not as deformable as ULW1. Many of the particles fail at about 0.2 effective strain. Young’s modulus for these particles is higher than those for ULW1. ULW3 particles are brittle; many particles fail below 0.2 effective strain. The Young’s modulus is the highest for ULW3 particles. The stress band in the middle of every plot shows stress range expected in Barnett shale. Young’s moduli are calculated from the above figures. At the room temperature, the Young’s modulus of ULW1 is around 15,400 psi. For ULW2, at the same temperature, this value is higher, at around 38,900 psi. ULW3 shows the highest value of Young’s modulus of around 41,100 psi. At the end of each test, the particles were closely inspected with naked eye. It was found out, ULW3 shattered into pieces confirming its brittle nature. ULW1 particles stayed intact. They got flattened with increasing stress, but never got broken into several pieces. ULW2 showed moderate deformability.

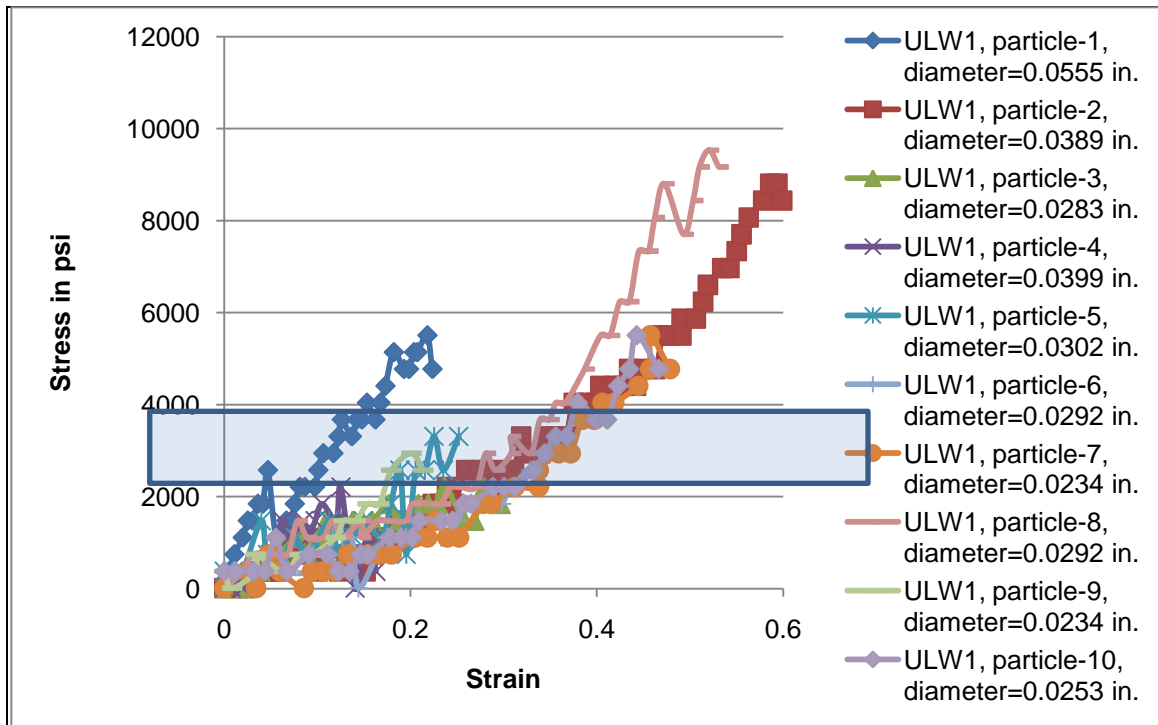


Figure 5.19 Elastic modulus of ULW 1 at ~25°C

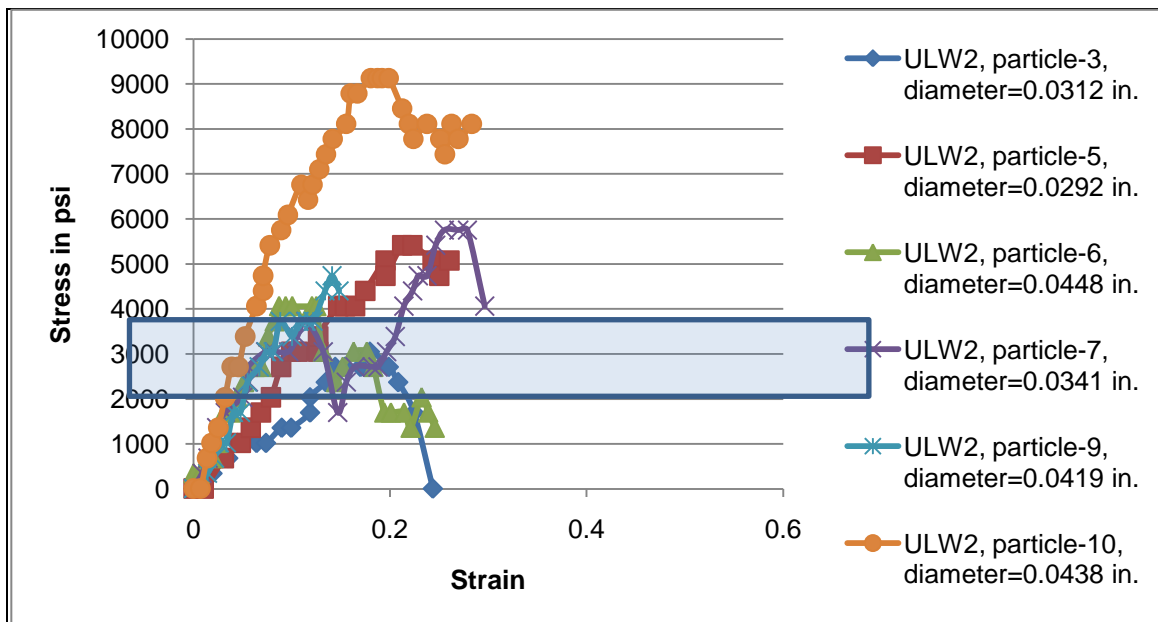


Figure 5.20 Elastic modulus of ULW 2 at ~25°C

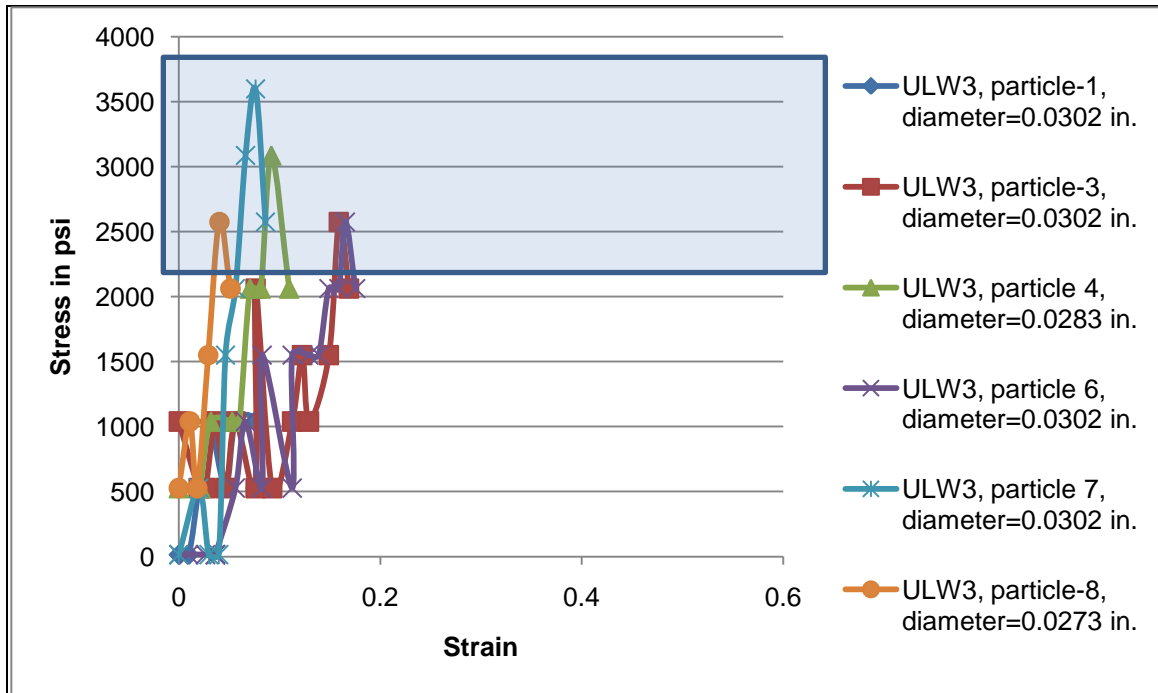


Figure 5.21 Elastic modulus of ULW 3 at ~25°C

5.6. CONDUCTIVITY TESTS

The long term conductivity of the proppant pack, at Barnett shale temperature of around 95 degrees, was measured under various levels of stresses (1000 psi, 2000 psi, 4000 psi and 6000 psi) following the guidelines of ISO 13503-5. Barnett shale is relatively hard and the problem of embedment of proppant is negligible. So in place of actual core plugs we can use hard steel shims which enclose the proppant pack at the top and bottom. Different concentrations of proppants (0.05 lbm/ft², 0.07 lbm/ft², 0.1 lbm/ft², 0.4 lbm/ft², 0.7 lbm/ft², 1 lbm/ft²) were tested during our study. Figure 5.22 shows the preliminary results for ULW1. It is evident in Figure 5.22 that a concentration of 0.05 lbm/ft² gives the same conductivity as 1 lbm/ft² for stress levels 4000 and 6000 psi. For lower stresses, 0.7 lbm/ft² and 1 lbm/ft² provide moderately higher conductivity than monolayer concentrations. For ULW2, concentration of 0.07 lbm/ft² or less creates a

partial monolayer between the fracture faces. A concentration of 1 lbm/ft² is more like a thick proppant pack. This study will be done at other concentrations too in the future. Figure 5.23 shows the preliminary results we got for ULW2. It is evident in the figure that a partial monolayer (0.07 lbm/ft²) provides as much conductivity as a thick proppant pack with a concentration of 0.7 lbm/ft². This is the one of the primary objectives of using ULWs, to create partial monolayer downhole between the fracture faces rather than thick proppant pack. Any concentration in between the thick proppant pack and the partial monolayer provides relatively smaller conductivity. ULW1 is lighter than ULW2, so a concentration other than 0.07 lbm/ft² (as compared to ULW2) will result in a partial monolayer. It is to be noted that ULW 1 and ULW 2 share a common feature of being deformable. So, these two kinds of proppants should behave similarly. If that is true, we should not expect the same kind of behavior from ULW 3, a less deformable and more brittle proppant type. So far, in this study, a partial monolayer of ULW 3 has not performed as efficiently as a thick pack of ULW 3. But, a partial monolayer of ULW 3 gives as much conductivity as monolayers of the other two proppants. A thick pack of ULW 3 is (10 times) more conductive than the thick packs of deformable proppant types (ULW 1 and ULW 2).

The conductivity of the partial monolayer proppant packs is in the range of 1-10 mD-ft. Brannon and Malone (2004) in their experiments achieved conductivity values as high as 100000 mD-ft for partial monolayers at 1000 psi confining stress. At a higher confining stress of 6000 psi, conductivity values they could achieve were around 1000 mD-ft. It is to be noted though; sandstone cores (with a certain permeability value) were used to enclose the proppant pack in all their tests. In the current study, the only possible flow path for the fluid was the actual proppant pack (with no cores). As pointed out earlier in this work, it is the dimensionless fracture conductivity (F_{CD}) which decides the

increase in productivity from any reservoir after the fracturing treatment. For a 10 nD reservoir, a fracture of length 100 ft and 1 md-ft conductivity would have a F_{CD} of 1000 which is large enough, as shown in Figures 2.1-2.4.

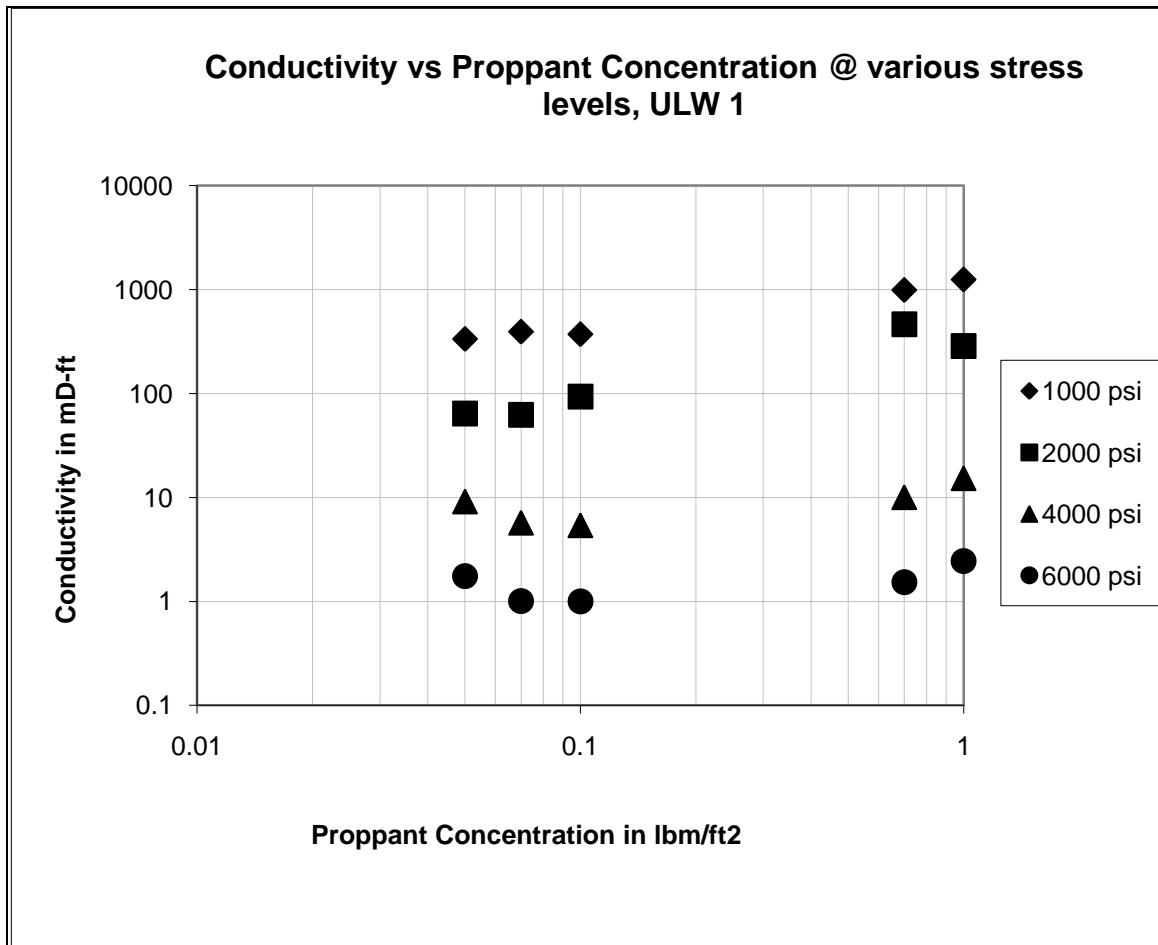


Figure 5.22 Fracture conductivity for ULW 1

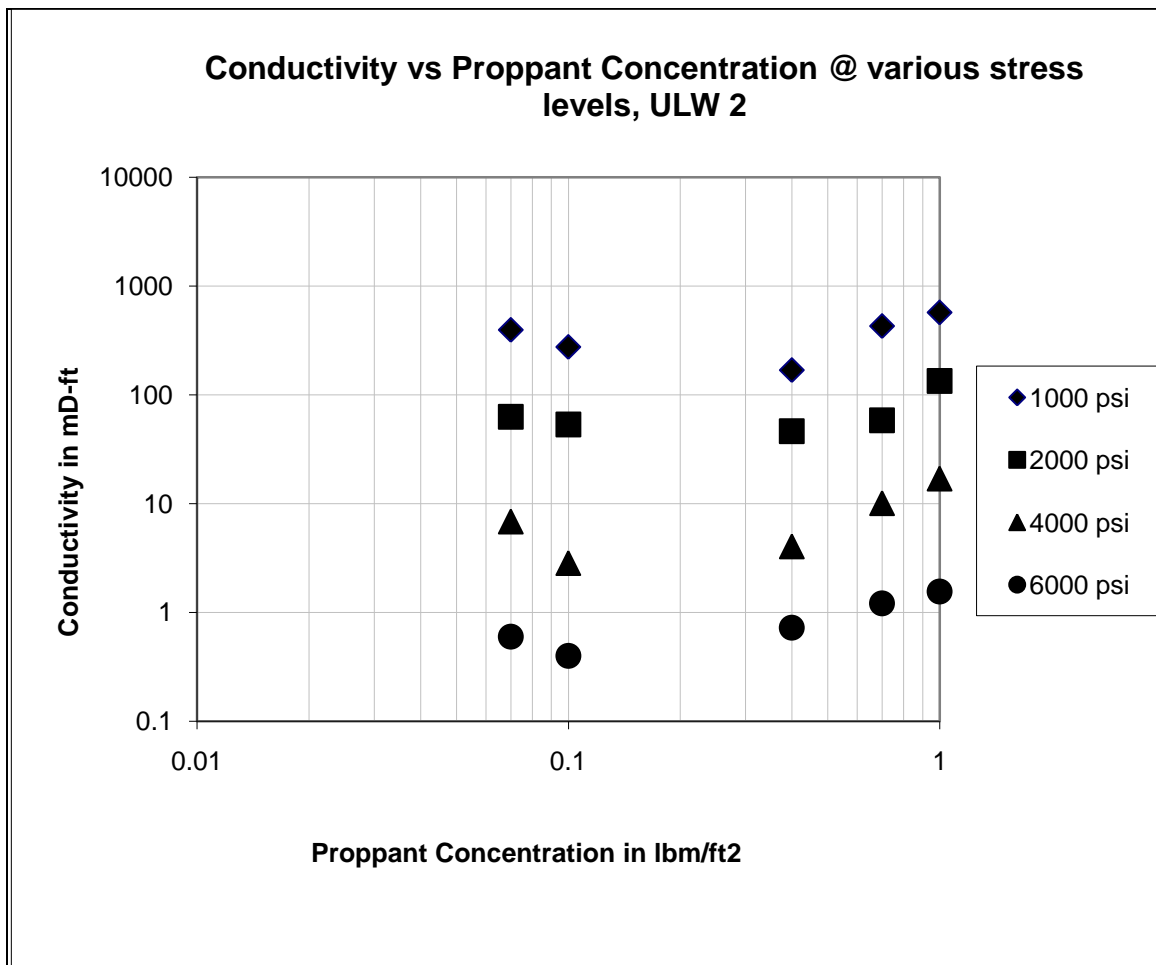


Figure 5.23 Fracture conductivity for ULW 2

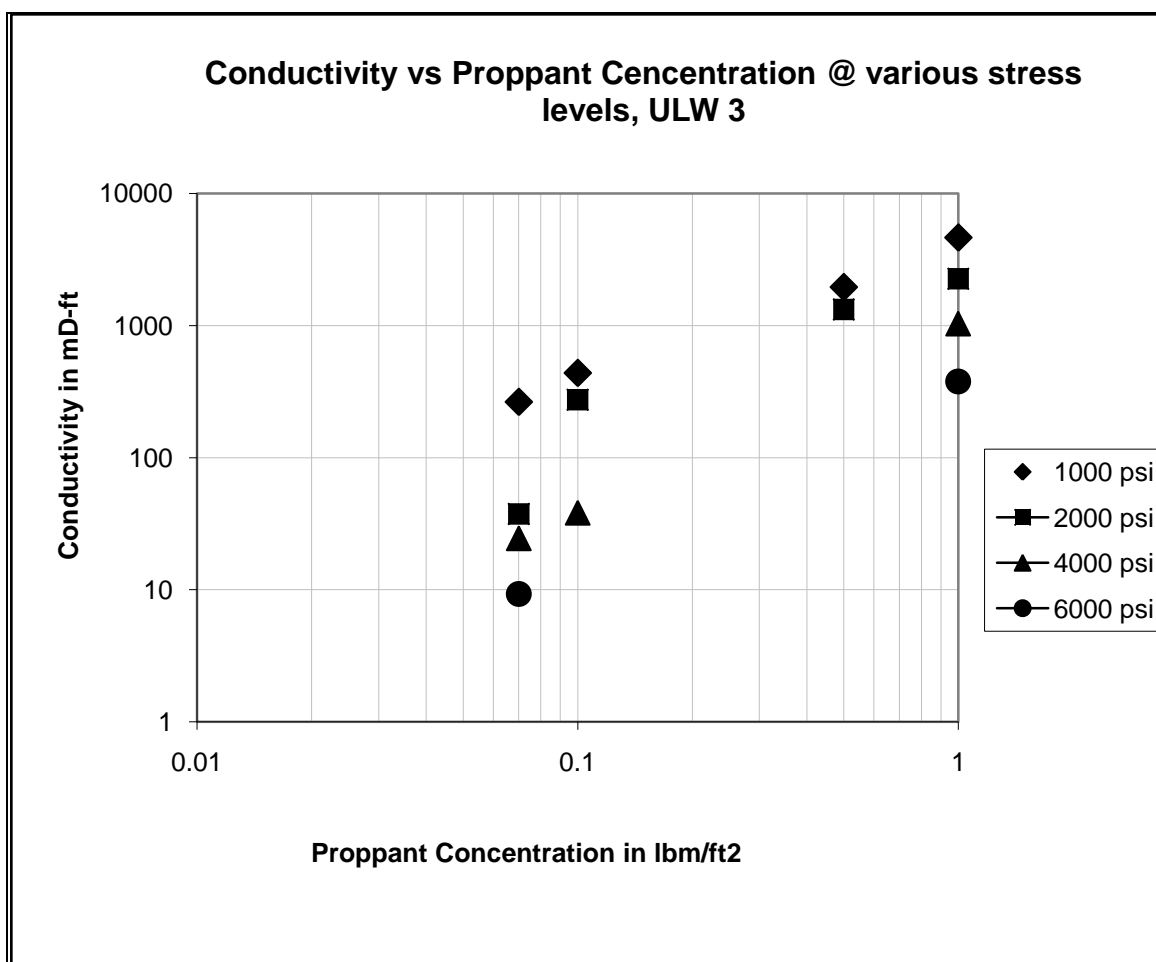


Figure 5.24 Fracture conductivity for ULW 3

6. Conclusions and Recommendations for Future Work

6.1. CONCLUSIONS

ULW 1 is spherical, ULW 2 is slightly angular and ULW 3 is highly angular. Bulk density of ULW 1 is the least (0.6 gm/ml); that of ULW 3 is the highest (1.2 gm/ml) and ULW 2 pack has an intermediate density (0.8 gm/ml). This means, for slickwater fracturing, transportability of ULW 1 is easier than the other two types of proppants. Of the three proppants tested, ULW 1 is the most deformable with the lowest effective young's modulus value of 15,400 psi. With the highest effective young's modulus value of 41,100 psi, ULW 3 is the most brittle. ULW 2 has an intermediate young's modulus value of 41,100 psi. ULW 1 and ULW2 lose less than 5% of proppants due to crushing of the proppant pack, whereas ULW 3 loses 15-30% proppants due to formation of fines. Of the three proppants tested, two of them, namely ULW 1 and ULW 2 were significantly strong to be able to endure the stresses (2000 psi-4000 psi) expected in the Barnett shale conditions as individual particles. The failure points of ULW 3 particles tested lay marginally above the expected stresses in Barnett shale. The proppant conductivity decreases as the confining stress increases. The decrease in conductivity is slightly lower for the partial monolayers than for the multilayered packs. The conductivity is a weaker function of the proppant concentration. A partial monolayer (0.07 lbm/ft^2) of ULW 2 provides slightly less or as much conductivity as a thick proppant pack with a concentration of 0.7 lbm/ft^2 . At 6000 psi stress, the conductivity of ULW 1 seems to decrease a little as the proppant concentration increases and then increases. This is due to the deformability of the proppant particles. For a monolayer, particles get deformed under stress, and there are spaces for fluid to flow around the particles. For a proppant pack of deformable particles, with increasing stress, the porosity and permeability of the whole pack decreases, thereby decreasing the overall conductivity of the proppant pack. For a

brittle proppant, like ceramic ULW 3, a partial monolayer is ten times less conductive than a thick pack. The thick pack of ULW 3 is 100 times more conductive than the thick packs of the other two proppants. The behavior of ULW 3 is more like a conventional proppant, the conductivity increases with the proppant concentration. The proppant conductivity is of the order of 1-10 md-ft, but this is high enough to stimulate shale formations of ultra low permeability.

6.2. RECOMMENDATIONS FOR FUTURE WORK

The use of actual shale cores in conductivity experiments will increase the applicability of the conductivity tests. These tests can easily be customized, according to the depth, stresses, temperature, hardness, and Young's modulus of the shale formation under consideration. Performance of same proppant in different reservoirs can be compared, by using the actual shale plugs from the reservoirs. The transportability of these light weight proppants relative to conventional proppants has to be tested separately in slot flow tests. Transport of proppants in the whole fracture network can be tested, by designing slots with lateral networks, which can open up under high pressure fluid. Eventually all these lab tests need to be followed up with field scale tests to see their actual performance.

References

- Aboud, R. S., and Melo, R. C. B., "Past Technologies Emerge Due to Lightweight Proppant Technology: Case Histories Applied on Mature Fields", SPE 107184, presented at the 2007 SPE Latin American and Caribbean Petroleum Engineering Conference held in Buenos Aires, Argentina, 15-18 April 2007.
- Asmolov, E. S., "The inertial lift on a small particle in weak-shear parabolic flow", *Physics of Fluids*, v. 14, No. 1, pp. 15, 2002.
- Bird, R. B., Stewart W. E., and Lightfoot, E. N., "Transport Phenomena, 2nd Edition" 2006.
- Brannon, H. D., Malone, M. R., Rickards, A. R., Wood, W. D., Edgeman J. R., and Bryant, J. L., "Maximizing Fracture Conductivity with Proppant Partial Monolayers: Theoretical Curiosity or Highly Productive Reality?", SPE 90698, presented at the SPE Annual Technical Conference and Exhibition held in Houston, Texas, U.S.A., 26-29 September 2004.
- Brannon, Harold. D., and Starks, Thomas. R., "Maximizing Return on Fracturing Investment by Using Ultra-Lightweight Proppants to Optimize Effective Fracture Area: Can Less Really Deliver More?", SPE 119385, presented at the 2009 Hydraulic Fracturing Technology Conference held in The Woodlands, Texas, USA, 19-21 January 2009.
- Britt, L. K., and Schoeffler, J., "The Geomechanics Of a Shale Play: What Makes A Shale Prospective!", SPE 125525, presented at the 2009 SPE Eastern Regional Meeting held in Charleston, West Virginia, USA, 23-25 September 2009.
- Cinco-L., H., Samaniego-V., F., and Dominguez-A., N.: "Transient Pressure Behavior for a Well With Finite-Conductivity Vertical Fracture, "Soc. Pet. Eng. J. (Aug 1978) 253-264.
- Darin, S.R. and Huitt, J.L.: "Effect of a Partial Monolayer of Propping Agent on Fracture Flow Capacity", SPE 1291-G, presented at the Annual Fall Meeting of SPE, Dallas, October 4-7, 1959.
- Economides, M. J., Hill D. A., and Ehlig-Economides, C., "Petroleum Production Systems" 2008.
- Folk, R. L., "Petrology of Sedimentary rocks", 1968
- Halliburton,
http://www.halliburton.com/public/solutions/contents/shale/related_docs/H063771.pdf.
- Howard, G. C., Fast, C. R.: "*Monograph 2 – Hydraulic Fracturing*", AIME, Millet the Printer, Dallas, TX (1970).

- Hudson, P. J., and Matson, R.P., "Hydraulic Fracturing in Horizontal Wellbores", SPE 23950, presented at the 1992 Permian Basin Oil and Gas Recovery Conference held in Midland, Texas, March 18-20, 1992.
- International Standard, "Measurement of properties of proppants used in hydraulic fracturing and gravel-packing operations", ISO 13503-2.
- International Standard, "Procedures for measuring the long-term conductivity of proppants", ISO 13503-5.
- Kaufman, P. and Penny, G. S., "Critical Evaluations of Additives Used in Shale Slickwater Fracs", SPE 119900, presented at the 2008 SPE Shale Gas Production Conference held in Fort Worth, Texas, U.S.A., 16-18 November 2008.
- Kundert, D., and Mullen, M., "Proper Evaluation of Shale Gas Reservoirs Leads to a More Effective Hydraulic-Fracture Stimulation", SPE 123586, presented at the 2009 SPE Rocky Mountain Petroleum Technology Conference held in Denver, Colorado, USA, 14-16 April 2009.
- Mcguire, W. J., and Sikora, V. J., "The Effect of Vertical Fractures on Well Productivity," *Trans., AIME* (1960) **219**, 401-03.
- Palisch, T. T., Vincent, M. C., and Handren, P. J., "Slickwater Fracturing: Food for Thought", SPE 115766, presented at the 2008 SPE Annual Technical Conference and Exhibition held in Denver, Colorado, USA, 21-24 September 2008.
- Rickards, A. R., Brannon, H. R., Wood, W. D., and Stephenson, C. J., "High Strength, Ultralightweight Proppant Lends New Dimensions to Hydraulic Fracturing Applications", SPE 84308, presented at the 2003 SPE Annual Technical Conference and Exhibition, Denver, 5-8 October.
- Rickman, R., Mullen, M., Petre, E., Grieser, B., and Kundert, D., "A Practical Use of Shale Petrophysics for Stimulation Design Optimization: All Shale Plays Are Not Clones of the Barnett Shale", SPE 115258, presented at the 2008 SPE Annual Technical Conference and Exhibition held in Denver, Colorado, USA, 21-24 September 2008.
- Schein, Gary. W., "The Application and Technology of Slickwater Fracturing", SPE 108807, SPE Distinguished Lecture, 2005.
- Shah, S. N., Lord, D. L., and Tan, H. C., "Recent Advances in the Fluid Mechanics and Rheology of Fracturing Fluids", SPE 22391, presented at the SPE International Meeting on Petroleum Engineering held in Beijing, China, 24-27 March 1992.
- Terracina, J. M., Turner, J. M., Collins, D. H., and Spillars, S. E., "Proppant Selection and Its Effect on the Results of Fracturing Treatments Performed in Shale Formations", SPE 135502-MS, presented at the SPE Annual Technical Conference and Exhibition, Florence, Italy, 19-22 September 2010.

- Tinsley, J. M. *et al.*: “Vertical Fracture Height-Its Effect on Steady-State Production Increase,” *JPT* (May 1969) 633-38; *Trans.*, AIME, **246**
- Wang, Fred. 2008. Production Fairway: Speed Rails in Gas Shale. Presented at the 7th Annual Gas Shale Summit, Dallas, Texas, 6-7 May.
- Wright, J. D., “Economic Evaluation of Shale Gas Reservoirs”, SPE 119899, presented at the 2008 SPE Shale Gas Conference held in Fort Worth, Texas, U.S.A., 16-18 November 2008.

Vita

Abhishek Gaurav was born in Patna, India on September 04, 1986, the son of G.S.Pandey and Sudha Pandey. He received his B.Tech in Mechanical Engineering from Indian Institute of Technology, Madras in 2008. In September 2008, he entered The Graduate School at The University of Texas.

E-mail: agaurav1986@gmail.com

This thesis was typed by the author.